

Brain Tumor Segmentation of MRI Images: A Comprehensive Review on the Application of Artificial Intelligence Tools

Ramin Ranjbarzadeh¹, Annalina Caputo², Saeid Jafarzadeh Ghouschi³, Erfan Babae Tirkolaee^{4,*}, Malika Bendeche⁵

¹ School of Computing, Faculty of Engineering and Computing, Dublin City University, Ireland.

ramin.ranjbarzadehkondrood2@mail.dcu.ie (corresponding author)

² School of Computing, Faculty of Engineering and Computing, Dublin City University, Ireland.

annalina.caputo@dcu.ie

³ Faculty of Industrial Engineering, Urmia University of Technology, Urmia, Iran.

s.jafarzadeh@uut.ac.ir

⁴ Department of Industrial Engineering, Istinye University, Istanbul, Turkey.

erfan.babae@istinye.edu.tr (corresponding author)

⁵ Lero & ADAPT Research Centres, School of Computer Science, University of Galway, Ireland.

malika.bendeche@universityofgalway.ie

Abstract

Background

Brain cancer is a destructive and life-threatening disease that imposes immense negative effects on patients' lives. Therefore, detection of brain tumors at an early stage improves the impact of treatments and increases patients' survival rate. However, detecting brain tumors in their initial stages is a demanding task and an unmet need.

Methods

The present study presents a comprehensive review of the recent Artificial Intelligence (AI) methods of diagnosing brain tumors using MRI images. These AI techniques can be divided into Supervised, Unsupervised, and Deep learning (DL) methods.

Results

Diagnosing and segmenting brain tumors usually begin with Magnetic Resonance Imaging (MRI) on the brain since MRI is a noninvasive imaging technique. Another existing challenge is that the growth of technology is faster than the rate of increase in the number of medical staff who can employ these technologies. It has resulted in an increased risk of diagnostic misinterpretation. Therefore, developing robust automated brain tumor detection techniques has been studied widely over the past years.

Conclusion

The current review provides an analysis of the performance of modern methods in this area. Moreover, various image segmentation methods in addition to the recent efforts of researchers are summarized. Finally, the paper discusses open questions and suggests directions for future research.

Keywords: Brain Tumor, Artificial Intelligence, Tumor Segmentation, Tumor Classification, MRI Modalities.

39 1. Introduction

40 Brain is an important organ containing one hundred billion nerve cells or neurons. According
41 to the reports, brain tumors are the 10th main cause of mortality among the adults and children for
42 both genders in developed countries [1], [2]. It is anticipated that the incidence of primary brain
43 tumors will cause 18280 deaths in adults in the USA in 2022 [3]. Brain tumors, known as
44 intracranial tumors, include a diverse set of cancerous cells that start in the intracranial tissues of
45 the brain and can range in malignancy from benign to advanced [4],[5]. Brain tumor begins in case
46 of cell division rates increase and multiply uncontrollably. Any portion of the brain or skull can
47 develop a brain tumor, including the brain's protective lining, skull base, brainstem sinuses, nasal
48 cavity, and many other places [6]. There are more than 150 kinds of brain tumors. The two basic
49 classifications of brain tumors are cancerous and noncancerous [7], [8].

50 The brain is made up of several cell types, each with its own special characteristics. It is
51 impossible to generalize results from malignancies in other organs to those arising in the brain [9].
52 The unique biology and microenvironment of the brain is the main aspect of brain cancers. Each
53 form of tumor has its own biology, course of therapy, prognosis outlook, and a different set of risk
54 factors [10], [11], and this makes the brain tumor classification difficult to describe. Pressure in
55 the head caused by a brain or spinal cord tumor is a common sign of brain cancer. People with
56 brain tumors are more likely to have specific symptoms, such as exhaustion, nausea, or discomfort.
57 The other side effects of living with brain tumors and brain cancer are fever, rash, and increased
58 pulse. The experts can link signs and symptoms to describe the problem with more certainty.
59 However, brain tumors do not always cause symptoms [12], [13].

60 Diagnosing a brain tumor involves three different tests and procedures, including imaging tests,
61 neurological exams, and biopsy. The most common and well-established method to diagnose brain
62 cancers is using Magnetic Resonance Imaging (MRI) [14]. During an MRI scan, a dye can be
63 injected into a vein. Experts assess the tumor and make treatment plans based on the MRI scan
64 elements, e.g., perfusion MRI, functional MRI, and magnetic resonance spectroscopy. In some
65 circumstances, further imaging tests like Positron Emission Tomography (PET) and Computed
66 Tomography (CT) are used in combination with MRI. Problems in any area can signify which part
67 of the brain is affected by a tumor [15], [16]. In this case, neurological tests can help the expert for
68 a better diagnosis. During the neurological examination, the expert checks the hearing, vision,
69 coordination, balance, strength, and reflexes of the patient. For a more precise diagnosis, a biopsy
70 is utilized. In this procedure, a sample of abnormal tissue collects and examined under the
71 microscope [17], [18].

72 If the practitioners can diagnose the disease early, it can result in a timely treatment which
73 increases the likelihood of survival. However, because tumor regions frequently have unclear
74 morphological structures, the identification of malignancies can be challenging [19]. Physicians
75 have recently used Computer-Aided Diagnostic (CAD) tools to aid in the diagnosis of cancer more
76 accurately [20]–[23]. These innovative methods of brain imaging have increased the detection ratio

77 of brain tumors [24]. Due to the requirement for intelligence in CAD systems, significant changes
78 have occurred recently, and Artificial Intelligence (AI) is integrated with CAD to reduce the
79 recognition time and system memory requirements [25], [26]. Also, it aids in the development of
80 a useful knowledge-based design system. Comparing the new AI assistance with the traditional
81 CAD system, one can realize that the new AI assistance, when combined with CAD, proves to be
82 more efficient. The accuracy and algorithms of AI systems have improved as a result of the
83 growing application of Deep Learning (DL) in medical research and the growth of big data
84 analytics. For example, a radiologist can apply the latest AI technology and advanced computer-
85 assisted detection and diagnosis to collect more details about the normal and tumor tissues [27].
86 Furthermore, it is possible to assess the patient's status by employing CADs and analyzing imaging
87 and/or non-imaging patient data. Over the last decades, this technology significantly influenced
88 early cancer detection and its timely treatment [28].

89 This review has summarized more than 100 scientific research papers from 2015- 2022 (until
90 1st September 2022). To find out the number of investigations on brain tumor diagnosis through
91 supervised learning, unsupervised learning, and DL models a statistical report is provided based
92 on the “Scopus” database. The keywords searched in this database were “brain tumor” AND “name
93 of the technique (e.g., Random Forest)” OR “brain cancer” AND “name of the technique”.

94 This paper focuses on reviewing the studies that applied AI techniques for brain tumor
95 segmentation. Abbreviations used in this paper are referenced in Table 1.

96 The rest of the paper is organized as follows: Detailed images of body organs in Magnetic
97 Resonance Imaging (MRI) is described in section 2. Different types of tumors and their
98 characteristics are implied in section 3. In section 4, more details about supervised and
99 unsupervised techniques are represented. Next, some Deep learning models applied in the field of
100 brain tumor segmentation are discussed in section 5. In the next step, some top databases for the
101 brain tumor segmentation are represented in section 6. Then, performance measures are described
102 in section 7. Finally, discussion and conclusion parts are provided in sections 8 and 9.

103
104
105

Table 1. List of abbreviations.

Description	Abbreviation	Description	Abbreviation
Magnetic Resonance Imaging	MRI	Cerebrospinal Fluid's	CSF
Artificial Intelligence	AI	Glioblastoma Multiforme	GBM
Positron Emission Tomography	PET	Low-Grade Glioma	LGG
Computed Tomography	CT	High-Grade Glioma	HGG
Computer-Aided Diagnostic	CAD	Radio Frequency	RF
Repetition Time	TR	Time To Echo	TE
Fluid Attenuated Inversion Recovery	FLAIR	Support Vector Machine	SVM
Artificial Neural Network	ANN	Random Forest	RF
K-Nearest Neighbors Algorithm	KNN	Linear Discriminant Analysis	LDA
Genetic Algorithm	GA	Maximum Marginal Hyperplane	MMH
Social Ski Driver	SSD	Kernel Support Vector Machine	KSVM
Random Decision Forest	RDF	Gaussian Mixture Model	GMM

Decision Tree	DT	Random Forest Classifier	RFC
Proton density	PD	Chemical shift imaging	CSI
Whale Optimization Algorithm	WOA	An Adaptive Artificial Neural Network	AANN
Fuzzy-C-Mean	FCM	Naive Bayes Classifier	NBC
Harmony-Crow Search	HCS	Particle Swarm Optimization	PSO
Learning Vector Quantization	LVQ	Self-Organizing Maps	SOM
Principal Component Analysis	PCA	Adaptive Kernel Fuzzy C-Means	AKFCM
Contrast Enhanced Fuzzy C-Means	CEFCM	Pixel-Based Voxel Mapping Technique	PBVMT
Multiscale Fuzzy C-Means	MsFCM	Gray-Level Co-Occurrence Matrix	GLCM
Edge Adaptive Total Variation Denoising Technique	EATVD	Imaging Mass Spectrometry	IMS
Hierarchical Cluster Analysis	HCA	Region Of Interest	ROI
Association Allotment Hierarchical Clustering	AAHC	Density-Based Spatial Clustering of Applications with Noise	DBSCAN
Gustafson-Kessel	(G-K)	Convolutional Neural Network	CNN
Enhancing Tumor	ET	Whole Tumor	WT
Tumor Core	TC	Recurrent Neural Network	RNN
Long Short-Term Memory	LSTM	Generative Adversarial Networks	GAN
Residual Cyclic Unpaired Encoder-Decoder Network	RescueNet	Sailfish Political Optimizer	SPO
Deep Belief Networks	DBN	Stacked Sparse Autoencoder	SSAE
Reinforcement Learning	RL	Gated Recurrent Unit	GRU
Density-Based Spatial Clustering	DBSCAN	Gaussian Mixture Models	GMM
Earthworm Optimization Algorithm	EWA	Monarch Butterfly Optimization	MBO
Harris Hawks Optimization	HHO	Moth Search Algorithm	MSA
Hunger Games Search	HGS	Runge Kutta Optimizer	RUN
Slime Mould Algorithm	SMA	Colony Predation Algorithm	CPA

106 2. Magnetic Resonance Imaging In Brain Tumor Detection

107 Clinicians can plan the most effective and practical treatment for patients involved with brain
108 cancer by obtaining information from several restorative diagnostic imaging technologies,
109 including MRI, PET, and CT [29]. However, better images of organs and soft tissues can be
110 produced using MRI. Using radio waves and strong magnetic fields, MRI releases detailed images
111 of body organs [30]. Compared to a CT scan or X-rays, MRI provides clearer images and it is a
112 better option when doctors should see soft tissues. Brain tumor location and size are determined
113 using imaging methods like MRI [8]. MRI images typify significant data about tissue
114 characteristics, for example, Proton density (PD), spin-lattice (T1), and spin-spin (T2) relaxation
115 durations, chemical shift imaging (CSI), and flow velocity. These facts allow for a more accurate
116 representation of brain tissue [31], [32]. MRI scans can acquire images with various contrasts using
117 various procedures or acquisition parameters. T1 weighted images with contrast material
118 Gadolinium (T1c) aid in distinguishing tumor borders from surrounding normal tissues. T2
119 weighted (T2) images are typically employed to provide an underlying assessment, identify

120 different tumor types, and distinguish cancers from normal tissues. No enhanced tumors are seen
 121 using the T2 weighted scan in axial viewing with FLAIR. Given these unique characteristics, MRI
 122 provides a decision-making advantage in investigations of brain tumors [12]. Table 2 indicates the
 123 four types of MRI images.

124
 125

Table 2. MRI image modalities [34].

Type	Feature
T1	T1-weighted MRI Calculate the tissue's T1 (longitudinal) relaxation time. Brighter tissue has shorter relaxation times.
T2	T2-weighted MRI Calculate the tissue's T2 (transverse) relaxation time. Longer relaxation times result in brighter tissue
T1c	T1 weighted images with contrast material Gadolinium. The signal for tumor increase
FLAIR	Fluid Attenuated Inversion Recovery MRI. Cerebrospinal fluid's (CSF) bright signal is suppressed. Can more accurately identify small hyper-intense lesions.

126 **3. Brain Tumor Types**

127 Brain tumor, sometimes referred to as an intracranial tumor, is an abnormal lump where cells
 128 are amassed to reproduce uncontrollably [35]. Currently, over 120 types of brain tumors are
 129 detected, two basic types of which are primary and metastatic. Primary brain tumors, also known
 130 as Meningioma, are tumors that develop from the brain's tissues or its immediate surroundings and
 131 account for more than 30% of all brain tumors [36]. Glial (consisting of glial cells) and non-glial
 132 (formed on or in the brain structures; i.e., nerves, glands, and blood vessels) primary tumors are
 133 classified as benign or malignant. Those tumors developed in other parts of the body, like the lungs
 134 or breast, and spread to the brain typically through the blood flow are referred to as metastatic
 135 brain tumors [37]. Malignant tumors with metastases are regarded as cancer. There are several
 136 types of brain tumors. Table 3 represents the most common brain tumors.

137
 138

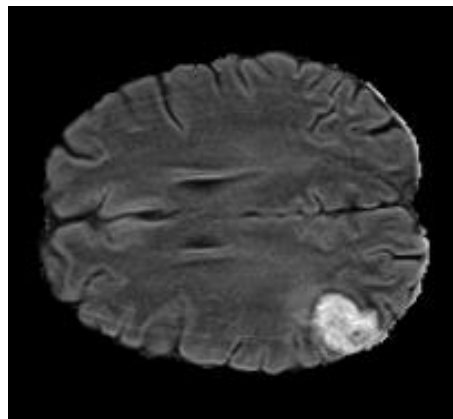
Table 3. Different types of brain tumors [38].

Brain Tumor Types		Subtype
1	Gliomas	Astrocytoma
2		Pilocytic Astrocytoma (grade I)
3		Diffuse Astrocytoma (grade II)
4		Anaplastic Astrocytoma (grade III)
5		Glioblastoma Multiforme (grade IV)
6		Oligodendroglioma (grade II)
7		Anaplastic Oligodendroglioma (grade III)
8		Ependymoma (grade II)

9	Anaplastic Ependymoma (grade III)
10	Craniopharyngioma
11	Epidermoid
12	Lymphoma
13	Meningioma
14	Schwannoma (neuroma)
15	Pituitary adenoma
16	Pinealoma (Pineocytoma, Pineoblastoma)

139
140
141
142
143
144
145

One of the most common types of brain cancer is Gliomas and account for almost 33% of all brain cancers [37], [39]. As gliomas frequently mix with healthy brain tissue and develop within the substance of the brain, they are sometimes referred to as intra-axial brain tumors. Glioblastoma, also named Glioblastoma Multiforme (GBM) and is challenging for experts to diagnose and cure. Fig. 1 shows the Glioblastoma imaging.



146
147

Fig. 1. MRI image of Glioblastoma.

148
149
150
151
152
153

Glioblastoma often has a blend of cell grades and changes synchronous to their growth. The features of tumors that appear under a microscope and the aggressiveness of the tumor make it possible for the experts to recognize tumor types. For example, if the grades are low, it means they are least aggressive, and if the grades are high, it indicates they are most aggressive. You can see the characteristics of Glioma scales in Table 4.

154

Table 4. Glioma grades and their characteristics [37].

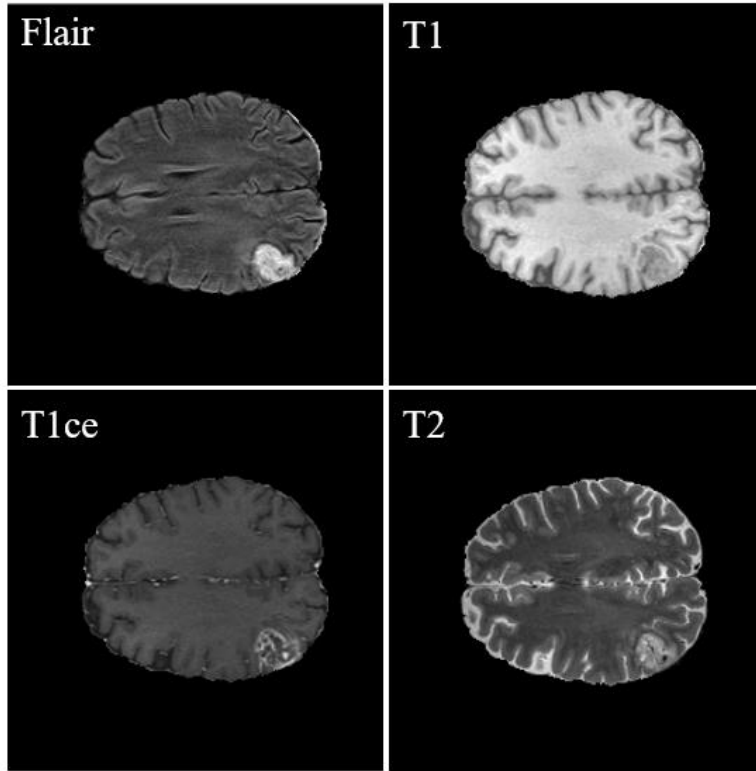
Grade	Characteristic
I	Near to normal appearance Least malignant Slow growing cells Commonly indicates long-term survival
II	Cells growing fairly slowly Fairly abnormal appearance Able to attack nearby tissue In some cases recur as a higher grade

III	Actively creating abnormal cells Abnormal appearance Infiltrate normal tissue Tend to recur, often as a higher grade
IV	Rapidly reproducing abnormal cells Highly abnormal appearance Area of dead cells (necrosis) in center Form new blood vessels to continue growth

155

156 In glioma, grades I and II (Table 4) are categorized as Low-Grade Glioma (LGG), and grades
157 III and IV are High-Grade Glioma or HGG [40]. Taking the best procedure for treatment depends
158 on the early diagnosis of Glioma and its grade [8], [37], and MRI imaging is one of the bests
159 screening methods for diagnosing Glioma. In this screening method, the protons which are
160 randomly oriented inside the water nuclei of the tissue are brought into alignment using a strong,
161 uniform, external magnetic field. The subsequent disruption of this alignment (or magnetization)
162 is caused by the addition of an external Radio Frequency (RF) energy. Through a variety of
163 relaxation mechanisms, the nuclei return to their resting alignment and release RF energy in the
164 process. The emitted signals are evaluated after a certain amount of time has passed from the first
165 RF. The signal from each place in the imaged plane is converted using the Fourier transform into
166 the relevant intensity levels, which are then represented as shades of gray in a matrix of pixels
167 [41]. Different forms of images can be produced by altering the order in which RF pulses are
168 delivered and collected. The T1- and T2-weighted scans are very popular MRI sequences. Short
169 Time to Echo (TE) and Repetition Time (TR) is utilized to create T1-weighted images. T1
170 characteristics of tissue are primarily responsible for determining the contrast and brightness of
171 the image. On the other hand, longer TE and TR times are used to create T2-weighted images. The
172 T2 characteristics of the tissue determine the contrast and brightness in these images. The Fluid
173 Attenuated Inversion Recovery (Flair) sequence is a third frequently utilized sequence. The TE
174 and TR timings of the Flair sequence are significantly longer than those of a T2-weighted image
175 [42]. Fig. 2 indicates the MRI image T1, T2, FLAR modalities.

176



177
178 **Fig. 2.** Some examples of MRI images including T1, T1ce, T2, and Flair.

179 Table 5 shows the frequently-used MRI sequences, along with an estimate of their TR and TE
180 times for different tissues.

181

182

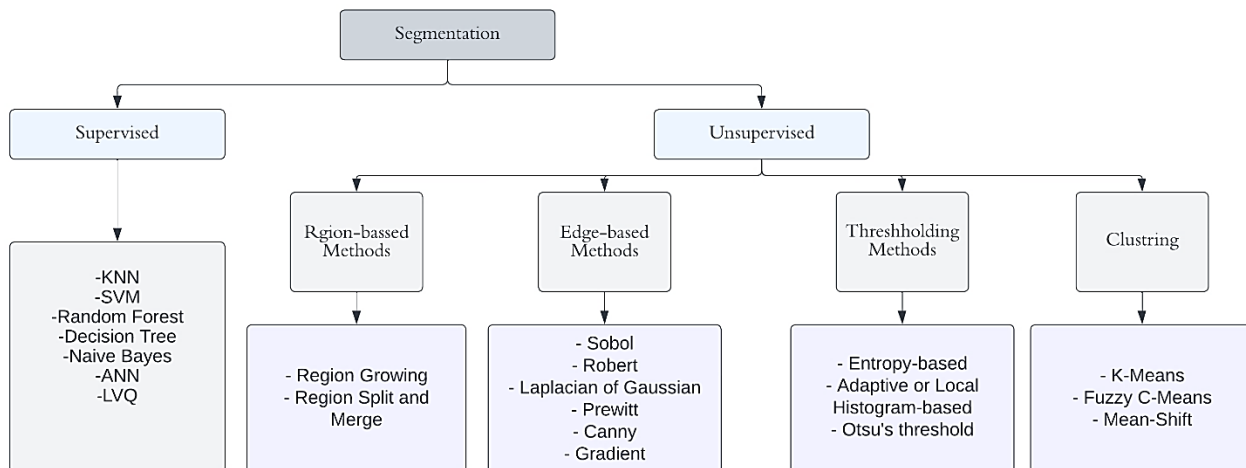
Table 5. Most common sequences of the MRI images [43].

Tissue	T1	T2	FLAIR
White matter	Light	Dark gray	Dark gray
CSF	Dark	Bright	Dark
Fat	Bright	Light	Light
Cortex	Gray	Light gray	Light gray
Inflammation	Dark	Bright	Bright

183 **4. Brain Tumor Segmentation**

184 Segmentation means grouping regions or pixels of images into many coherent subregions and
185 categorizing each subregion into one of the specified classes based on the extracted features, such
186 as color or texture attributes [44]–[46]. Segmentation is a form of image compression and has
187 extensive applications in the development of CAD that works based on radiological images such
188 as MRI. Generally, image segmentation can be categorized into two main groups: supervised and
189 unsupervised [47]–[49]. Unsupervised segmentation approaches include thresholding, edge
190 detection, graph cutting, and deformation to define the boundaries of the target item in the image
191 [50], [51]. In contrast, supervised segmentation techniques apply training samples to include prior

192 knowledge about the image processing problem. Fig. 3 shows the categories of supervised and
 193 unsupervised approaches.



194
 195

Fig. 3. Brain tumor segmentation approaches.

196 To find out the number of investigations on brain tumor diagnosis through supervised and
 197 unsupervised learning, a statistical report is provided based on the “Scopus” database. The
 198 keywords searched in this database were “name of the method (e.g., SVM)” AND “brain tumor”
 199 OR “name of method” AND “brain cancer.” The date of publication was set from 2015- 2022
 200 (until 1st September 2022). Fig. 4 shows the number of publications that used Machine Learning
 201 (ML) approaches to diagnose brain cancer. According to Fig. 4, “Support Vector Machine
 202 (SVM),” with 1136 papers published between 2015 to 2022, is the most used approach for brain
 203 tumor classification or segmentation. This approach is employed in two ways, directly applied to
 204 databases or used in a hybrid with other techniques. SVM, more than 90% of the time, indicated a
 205 high accuracy rate, and this is the main reason for the highest number of publications based on this
 206 approach. The second approach that is applied to diagnose brain tumors is “Artificial Neural
 207 Network (ANN)”. The number of investigations conducted based on this approach is about 846
 208 papers. Random forest is the third popular approach with 834 papers. In the following, the ML
 209 approaches are introduced briefly and the several papers that applied the approach are discussed.

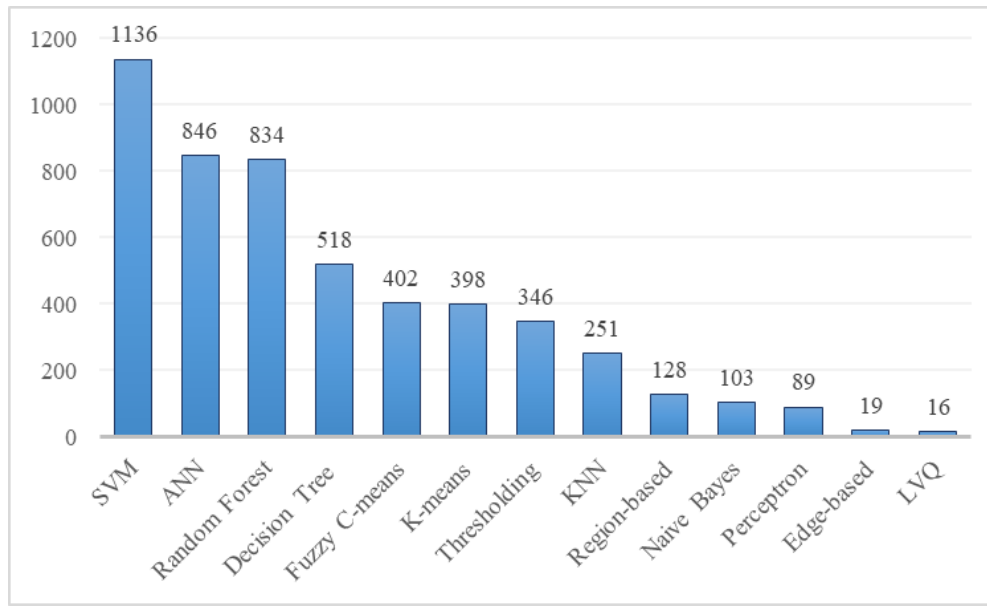


Fig. 4. Number of publications between 2015 to 2022 for brain tumor segmentation using supervised and unsupervised learning techniques.

4.1 Supervised Learning

Supervised learning is a popular branch of ML algorithms and commonly is referred to as supervised ML. In this approach, labeled datasets are utilized to train computers in order to properly categorize data or predict outcomes [52], [53]. The model modifies its weights until the model is properly fitted, which is a part of the cross-validation process. A training set is used in supervised learning to instruct patterns to produce optimal results. This training dataset has accurate input data and outputs (labels), enabling the model to develop through time. The algorithm evaluates precision using the loss function and modifies it to minimize the error. Supervised learning techniques assist in finding large-scale solutions to real-world issues, including in the medical field. Various methods of supervised learning have been applied to diagnose a brain tumor. In the following, a list of techniques is provided.

The most important benefit of these methods is that they allow to produce a data output or collect data from the prior experience. The main disadvantage of these models is inability to correctly classify an input data that was not belonged to any classes in the training data.

4.1.1 K-nearest Neighbors Algorithm

The K-Nearest Neighbors (KNN) algorithm is a supervised learning classifier that employs proximity for classifications or predictions about the grouping of a data point [54]. Although it can be applied to classification or regression issues, it is commonly employed as a classification method since it relies on the concept that similar points can be discovered near one another [55]. It is also known as a lazy learner algorithm. KNNs have been common in brain cancer segmentation, and the results of studies had different accuracy rates. For example, Havaei et al.

235 [56] created a structure for interactive brain tumor segmentation and applied it to MICCAI-BRATS
236 2013. This study suggested a semi-automatic method to enhance the effectiveness of various
237 classification techniques, including SVM, KNN, and random forests. The improved KNN reported
238 85%, 91%, and 87% for accuracy, specificity, and sensitivity rates, respectively. But SVM
239 outperformed and yielded better rates.

240 Çınarler et al. [57] investigated the statistical features of the input images in order to categorize
241 the data. Then, a variety of methods were employed to examine the accuracy rate of various ML
242 algorithms, including KNN, LDA (linear discriminant analysis), RF (random forest), and SVM.
243 However, KNN's accuracy rate was lower than SVM's 90% accuracy rate. Kumar et al. [58]
244 proposed a four-modular framework that employed an adaptive KNN classifier to categorize MRI
245 images of brain tumors into normal or abnormal categories. Then, the optimal probabilistic Fuzzy
246 C-Means (FCM) clustering approach is applied to separate the tumor areas. The application of the
247 proposed work on BRATS MICCAI dataset indicated the evaluation's findings show that the
248 suggested technique, which employs KNN-based brain tumor classification, achieved the highest
249 accuracy of 96.5%. The maximum sensitivity was 100%, while the maximum specificity was 93%.
250 Ajai et al. [59] performed analyses on various pre-processing algorithms that can be utilized to
251 enhance images prior to applying the active contour without performing the technique called edge-
252 based segmentation. Moreover, both the linear kernel SVM and KNN classifiers' accuracy were
253 compared. According to the findings, KNN is superior to linear SVM for classifying brain tumors
254 when active contouring without an edge-based method of segmentation is utilized.

255 In order to identify and categorize the different types of tumors, Ramdlon et al. [60] created a
256 tumor classification system based on the KNN method that can identify tumors and edema in T1
257 and T2 imaging sequences. The tumor categorization reported 89.5% in terms of accuracy, which
258 can give more precise and detailed information about tumor detection. For the classification of
259 glioblastoma, Wibowo et al. [61] compared the use of KNN and SVM methods. Additionally, the
260 Genetic Algorithm (GA) was applied to identify the chosen relevant features and categorize them
261 using KNN and SVM techniques. With 92.35 percent accuracy, the findings demonstrated that the
262 SVM-GA method outperformed the KNN-GA strategy.

263 Although the KNN technique is much faster than other strategies that require training (such as
264 decision tree, random forest, and SVM), but It does not learn anything in the training period (Lazy
265 Learner). Moreover, as the KNN technique doesn't need any training dataset before making
266 estimation, new input training samples can be added without impacting the performance of the
267 model.

268 *4.1.2 Support Vector Machines*

269 SVMs are effective and adaptable supervised ML algorithms used for both classification and
270 regression. However, they are typically implemented for classification. An SVM model is just a
271 hyperplane in a multidimensional space that represents two or more classes. SVM will construct
272 the hyperplane in an iterative manner in order to reduce error [62]. An SVM technique aims to
273 classify samples in order to identify a Maximum Marginal Hyperplane (MMH). As a result of its

274 flexibility in handling several continuous and categorical variables, SVM methods are widely-used
275 ML techniques [63], especially for brain cancer segmentation and classification. For example,
276 Amin et al. [64] developed an automated approach to identify brain tumors whether malignant or
277 benign in MRI images. To compare the proposed framework's precision, an SVM classifier was
278 applied with various cross-validations on the features set. The approach obtained average
279 accuracy, sensitivity, and specificity of 97.1%, 91.9%, and 98.0%, respectively.

280 Padlia et al. [65] suggested a method for identifying and segmenting brain tumors using T1-
281 weighted and FLAIR brain images. In order to enhance images and remove noise, a fractional
282 Sobel filter is utilized. Bhattacharya coefficients and mutual information are employed for
283 detecting asymmetry in brain image. After extracting features of the region of interest through the
284 windows and patches, SVM is used to categorize the statistical features to separate the tumor area
285 from the tumor hemisphere. Their method gained an average accuracy of 98.03%. In another study,
286 Khairandish et al. [66] presented a hybrid model, which integrated CNN and SVM models for
287 classification. Also, a threshold-based algorithm for detecting the brain tumor. The hybrid CNN-
288 SVM got a 98.49% overall accuracy. Rao and Karunakara [67] focused on efficient classification
289 and segmentation, using KSVM-SSD for more accurate classification. In this study, the malignant
290 tumor is further graded as a low, medium, and high utilizing the SSD (Social Ski Driver)
291 optimization method after being diagnosed as cancerous and non-cancerous using Kernel Support
292 Vector Machine (KSVM). The proposed KSVM-SSD model is shown to be superior regarding
293 classification accuracy assessed on the BRATS datasets, with accuracy values of 99.2%, 99.36%,
294 and 99.15% for the corresponding years of 2018, 2019, and 2020 BRATS datasets.

295 Rashid et al. [68] aimed to shed some light on the area of the brain being damaged by the tumor.
296 The major steps of the described technique include using abnormal MRI brain images as input,
297 anisotropic filtering to remove noise, an SVM classifier for segmentation, and morphological
298 procedures to distinguish the damaged area from the normal one. The results indicated that the
299 segmentation accuracy of the SVM was 83%. For the categorization of medical images, Deepak
300 & Ameer [69] applied CNN features with SVM to enhance the quality of classification. In
301 comparison to the most recent technique, the proposed model outperformed with 95.82% accuracy.

302 Although SVM is able to work well with even semi structured and unstructured data using an
303 appropriate kernel function, but finding a good kernel function is not an easy task.

304 *4.1.3 Random Forest*

305 Random Forest (RF) strategies are a collection of ML algorithms paired with several classifier
306 trees. Each classifier tree casts a unit vote for the most popular class, and the final sort of result is
307 obtained by combining these results [70]. High classification accuracy, good noise and outlier
308 tolerance, and no overfitting are all features of RFs. In addition to building each tree from a
309 separate bootstrap sample of the data, the RF technique modifies how classification or regression
310 trees are built [71]. In an RF model, node splitting is based on a random subset of features for each
311 tree. By comparing this counterintuitive approach to many other classifiers, it turns out to perform
312 very well. Therefore, this technique has been widely employed for brain cancer tumors. For

313 example, Lefkovits et al. [72] developed and fine-tuned a discriminative RF model to segment
314 brain tumors in multimodal MRI images. Finding the optimal parameter values and the
315 discriminative model's most important constraints is the goal of tuning. The proposed method
316 obtained 75-91% for the whole tumor and 71-82 % for the core section in terms of dice index.
317 Ellwaa et al. [73] expanded a previously described Random Decision Forest (RDF) based brain
318 tumor segmentation technique. The RDF is trained via an iterative process, where certain patients
319 were introduced to the training data using heuristics approaches rather than a randomly selected
320 training dataset. The obtained dice score of the model was reported to be over 80%.

321 Anitha & Raja. [74] introduced brain tumor identification and segmentation methods based
322 on random forest classifiers to classify the brain modality into two groups of normal and abnormal.
323 The proposed approach's sensitivity and specificity rates were 97% and 98%, respectively. Yang
324 et al. [75] utilized Small Kernels of Two-Path Convolutional Neural Network (SK-TPCNN) and
325 RF to provide an automated segmentation approach. The sensitivity scores for the whole tumor,
326 core tumor, and enhancing tumor were 96%, 92.2%, and 83.2%, respectively. Rajagopal. (2019)
327 suggested an approach based on a random forest classifier to detect the Glioma brain tumor. In this
328 study, the characteristics of texture are extracted from MRI images of the brain and optimized
329 using Ant Colony Optimization (ACO) algorithm. The resulting optimized sets of characteristics
330 were categorized thanks to the random forest classification method. The result of this study
331 indicated 97.7% of sensitivity, 96.5% of specificity, and 98.01% of accuracy [76].

332 Although RF helps to improve the accuracy by diminishes overfitting in decision trees and
333 works well with both continuous and categorical data, but it requires much time for training.

334 *4.1.4 Decision Tree*

335 Decision tree models (DTs), i.e., non-parametric supervised learning techniques are used in
336 regression and classification. The objective is to learn simple decision rules derived from the
337 features of the data to build a model to predict a target variable's value. One can assume a tree as
338 a piecewise constant approximation [77], [78]. The tree is utilized to let individuals or
339 organizations evaluate probable actions against each other based on their benefits, costs, and
340 probabilities. A single node is the starting point of a decision tree, which then forks into probable
341 outcomes. Then, every single outcome results in additional nodes, which lead to other probabilities
342 [79]. Previous studies have employed DT approaches for brain cancer diagnosis. For example,
343 Naik and Patel [80] applied a Decision Tree algorithm to discern brain tumors in MRI images and
344 compared the results with a Naive Bayes classification algorithm. The researchers reported that
345 the Decision Tree classifier outperformed a Naive Bayes in the task with an accuracy of 96% and
346 sensitivity of 93%. Chaddad et al. [81] implemented Gaussian Mixture Model (GMM) to take out
347 attributes from brain tumors' MRI images and applied the Decision Tree classifier to GMM
348 features to evaluate the performance of cancer detection. They defined the task to detect brain
349 tumors based on the T1, T2, and FLAIR MRI images. For the T1 and T2 weighted images, the
350 accuracy performance was 100 %. The accuracy decreased to 94.11 % in FLAIR mode. Hussain
351 et al. [82] implemented multiple feature extraction strategies on MRI images of the brain and so

352 tested the performance of different classification algorithms for tumor detection. The researchers
353 reported that the Decision Tree classifier was the second-best algorithm for the task with a total
354 accuracy of 97.81%, after the Naïve Bayes classifier with total accuracy of 100%.

355 Thayumanavan and Ramasamy [83] developed a framework for the diagnosis and segmentation
356 of tumors in the brain using MRI images and compared the performance of Decision Tree (DT),
357 Random Forest Classifier (RFC), and SVM. The experimental results showed that RFC reached
358 the best result with an accuracy of 98.37%. Moreover, RFC showed a specificity of 99.09%,
359 followed by DT and SVM with 95.68% and 88.78% respectively. Rajendran and Madheswaran
360 [84] developed a hybrid method based on Association Rule Mining and Decision Tree algorithms
361 for brain tumor classification using CT scan images. They showed that the proposed method
362 reached the accuracy and sensitivity of 95% and 97%, respectively.

363 Although DT doesn't need scaling and normalization of data, but it requires much time for
364 training. Also, a small change in input data leads to large changing in the structure of the model.

365 *4.1.5 Artificial Neural Network*

366 An ANN is a paradigm for information processing that takes its ideas from how biological
367 nervous systems can learn target patterns. Multiple layers of basic processing units known as
368 neurons make up an ANN structure [85]–[87]. The neuron carries out two tasks: gathering inputs
369 and producing an output. Nodes or artificial neurons are connected to other nodes together with
370 their threshold and weight. When the output of a node is higher than a certain threshold value, that
371 node is activated, and the data is sent to the next layer of the network. Otherwise, data won't be
372 sent to the next layer [88]. ANN has been widely-used for brain cancer. An SVM and an ANN
373 were utilized by Chithambaram and Perumal [89] to create two hybrid ML models (GA-SVM and
374 GA-ANN), which were then evaluated on two different datasets. Virupakshappa & Amarapur [90]
375 developed a technique for classifying data based on an Adaptive Artificial Neural Network
376 (AANN) approach. Utilizing the Whale Optimization Algorithm (WOA), the values of neurons in
377 the adaptive ANN are optimized. The result of classification accuracy was reported at 98%.
378 Virupakshappa et al. [91] suggested an effective tumor segmentation model based on FCM
379 clustering, multiple feature extraction using Gabor wavelets, and an ANN classifier. Based on the
380 result of this study, it is proved that system accuracy levels up to 85%.

381 Although an ANN model is able to process unorganized data, an effective visual analysis, and
382 ability to process in parallel, but it is economically and computationally expensive and needs a
383 long training process.

384 *4.1.6 Naïve Bayes*

385 A collection of supervised learning algorithms, Naïve Bayes methods, are founded on
386 implementing Bayes' theorem with the "naive" assumption that each pair of characteristics is
387 conditionally independent given the value of the class variable [92], [93]. Bayes' Theorem is a
388 straightforward mathematical procedure for conditional computing probabilities. Conditional
389 probability is defined as the possibility of an event occurring due to the occurrence of another

390 event before it (via assumption, supposition, statement, or evidence). The Naive Bayes Classifier
391 (NBC) is among the easiest and most efficient classification algorithms. It helps develop rapid ML
392 models, which can make accurate predictions [94]. There are several researches that applied Naive
393 Bayes to diagnose brain cancer in medical images. For example, Kaur and Oberoi (2019) applied
394 a Naive Bayes classifier to discover brain tumors in MRI images. The proposed algorithm showed
395 86% accuracy for brain tumor segmentation [95].

396 Raju et al. [96] implemented a Bayesian fuzzy clustering algorithm for the segmentation and
397 the Harmony-Crow Search (HCS) optimization algorithm-based multi-SVNN classifier for the
398 classification of brain tumors. The researchers reported that the proposed method reached an
399 accuracy of 93%. Ulku and Camurcu [97] utilized histogram equalization and morphological
400 image processing techniques to develop a computer-aided brain tumor detection method based on
401 MRI images. Six different classification algorithms were tested. Based on the final results, SVM-
402 PSO and KNN algorithms reached 100% accuracy. The Decision Tree algorithm showed 98.11%
403 accuracy in negative samples, while Naive Bayes showed the weakest performance with 83.71%
404 accuracy in negative samples.

405 Although Naive Bayes methods are appropriate for solving multi-class prediction problems and
406 require much less training data, but they face the ‘zero-frequency problem’ where they assign zero
407 probability to a categorical sample whose class in the test samples wasn’t available in the training
408 samples.

409 *4.1.7 Learning Vector Quantization*

410 The Learning Vector Quantization (LVQ) is a prototype-based supervised classification
411 algorithm. With the use of piecewise linear decision surfaces, this algorithm aims to approximate
412 the theoretical Bayes decision boundaries in the input domain of the principal observation vectors
413 [98]. The class codebook vectors are supposedly placed in signal space in an ideal manner. As the
414 classification decision is based on the nearest-neighbor selection among the codebook vectors, its
415 computation is very fast. LVQ algorithms have things in common with other competitive learning
416 algorithms, including Self-Organizing Maps (SOMs) and c-means [99]. This method has been
417 widely used for analyzing medical images and some researchers employed the LVQ approach for
418 brain tumor detection. For example, Liu et al. [100] employed the LVQ neural network for the
419 brain cancer prognosis. A normal diagnostic accuracy of 85.7% and a glioma diagnosis accuracy
420 of 89.5% were achieved by using the suggested procedure. Sonavane et al. [101] proposed a proper
421 and precise classification system for brain tumor detection. This technique uses the LVQ approach
422 to group brain tumors into two groups of normal or abnormal. With respect to the DDSM
423 mammography database and the clinical brain MRI database, the suggested system's accuracy was
424 68.85% and 79.35%, respectively. Sonavane & Sonavane [102] developed a four-stage system and
425 classified brain tumors using the Adaboost technique and LNQ neural network. For clinical brain
426 MRI images, the accuracy rate was 95%, while it was 79.3% for DDSM.

427 The LVQ is intuitive, simple, and easy to implement while still yielding decent performance.
428 However, if the data have a lot of dimensions or are noisy, the Euclidean distance is not a good
429 solution.

430 **4.2 Unsupervised Learning**

431 Unsupervised learning, as known as unsupervised ML, analyzes and groups unlabeled datasets
432 using ML algorithms. These algorithms cluster data and discover hidden patterns without the
433 intervention of a human [103]–[105]. In other words, unsupervised learning algorithms work based
434 on finding similar attributes, naturally occurring patterns and trends, or relationships in a given
435 dataset [106], [107]. In contrast to supervised learning, it is not possible to apply unsupervised
436 learning methods directly to a regression or a classification problem because there is no knowledge
437 about the values of the output [108]. Unsupervised learning algorithms enable to do more complex
438 processing tasks than supervised learning does. Moreover, dimensionality can be easily reduced
439 thanks to this approach. Unsupervised learning can help to understand raw data. This learning
440 resembles human intelligence as it happens gradually and weighs the result afterwards. Clustering
441 is an unsupervised method that clusters the data into a number of groups. There are many clustering
442 approaches that have been widely used in the medical imaging area, especially clustering brain
443 tumors into a benign and malignant one.

444 Unsupervised learning methods have less complexity in comparison with supervised learning
445 and don't require to labeled data. However, the outcomes often have lesser accuracy and may be
446 difficult to understand or unpredictable.

447 *4.2.1 K-means*

448 As a clustering method, K-means is a simple and well-liked algorithm of unsupervised ML
449 [109]. K-means clustering algorithm is prototype-based and seeks to find K non-overlapping
450 clusters. This approach aims to categorize a given collection of data into K distinct clusters, where
451 k has a predetermined value [110]. Benefiting from linear time complexity, K-means algorithm is
452 optimal for large datasets. K-means uses big unlabeled data to provide deep insights and be
453 beneficial. K-means have been employed in many investigations for brain tumor diagnoses. For
454 example, Khilkhali et al. [111] applied K-means clustering, thresholding, and morphological
455 operations, for segmenting brain tumors in MRI images. The morphological procedure removed
456 non-brain tissue to increase the final accuracy results. The experiments were implemented on
457 BRATS datasets utilizing High-Grade Glioma (HGG) and LGG images. Islam et al. [112]
458 proposed an improved outline to detect brain tumors that makes use of Template-based K-means
459 (TK) with a superpixel technique and Principal Component Analysis (PCA) in order to detect brain
460 tumors efficiently. Their method could obtain an acceptable segmentation result with a shorter
461 processing time in MRI images. Kumar et al. [113] proposed a five stages methodology to segment
462 brain tumors in MRI image segmentation. A rough K-means algorithm was used to achieve this
463 aim. The results are indicative of the fact that the suggested methodology gained better scores in
464 evaluation in comparison with previous works.

465 The K-means model is simple, easy to implement, and Guarantees convergence. However, it is
466 highly dependent on initial values and clustering outliers.

467

468 *4.2.2 Fuzzy C-Means*

469 Another well-known technique to cluster data is FCM where datasets are classified into n
470 clusters and is frequently used for pattern recognition [114]. Every segmented data point in the
471 dataset belongs to over one group with distinctive values for membership. If the data is closer to
472 the cluster center, its membership inclines more toward that particular cluster center [115].
473 Enabling memberships of data points through time may be the main benefit of FCMs clustering.
474 These data points are known to have degrees in $[0,1]$ and this technique makes it possible to show
475 that data points do not necessarily belong to one cluster. Moreover, FCM can provide the best
476 result for the overlapped data set [116]. Devi et al. [117] developed a clustering method called
477 Adaptive Kernel Fuzzy C-Means (AKFCM) for diagnosing brain cancer based on MRI images.
478 Then, they applied a Hybrid Convolution Neural Network- Long Short-Term Memory (CNN-
479 LSTM) to enhance the accuracy of tumor categorization. The results indicated that the proposed
480 method did better than the present methods.

481 Debnath et al. [118] applied the Contrast Enhanced Fuzzy C-Means (CEFCM) clustering
482 method to accurately categorize the 2D tumor regions from MR images. Pixel-based Voxel
483 Mapping Technique (PBVMT) mapped the decision values for each pixel location from the
484 segmented image into 3D space and showed the overall accuracy, sensitivity, and specificity of
485 94.8%, 92.14%, and 96.97%, respectively. Sheela et al. [119] proposed a method to segment brain
486 tumors in MRI images based on rotating triangular sections with FCM optimization. At first, the
487 background should mostly be eliminated through morphological reconstruction processes in two
488 levels, after which thresholding happens. To assess the proposed structure's performance, they
489 employed T1-a weighted contrast-enhanced image dataset. The final assessment of the proposed
490 method is indicated. Soleymanifard et al. [120] applied a classification method, which was a
491 Multiscale Fuzzy C-Means (MsFCM) with 12 scales to discern enhancing tumors in the image
492 cropped from the former stage. Then, thanks to using a neural network classifier, they managed to
493 specify the input tumors' grade in the MR image. The DICE score results show that the model
494 proposed is highly competitive in comparison with newer segmentation methods.

495 The Fuzzy C-Means model gains best results for overlapped sample points and comparatively
496 better than k-means strategy. However, it is highly dependent on the predefined number of clusters.

497 *4.2.3 Mean-Shift Clustering*

498 Mean shift clustering algorithm is a powerful nonparametric technique based on centroid that
499 is proven to be useful in various unsupervised learning use cases [121], [122]. This algorithm
500 works by moving data points toward centroids to become the average of nearby points. Mode-
501 seeking algorithm is another name for mean shift clustering. The algorithm's advantage is that it
502 clusters the data without automatically determining how many clusters there should be based on
503 defined bandwidth [123]. Researchers have implemented mean-shift clustering for the clustering

504 of brain tumors. Vallabhaneni and Rajesh [124] developed a method based on mean-shift
505 clustering, and Gray-level Co-Occurrence Matrix (GLCM) features for automatically diagnosing
506 brain tumors in noise-corrupted images. The researchers implemented Edge Adaptive Total
507 Variation Denoising Technique (EATVD) for preserving the edges in the denoising process of
508 images. The experimental results showed an increased precision in tumor detection in noisy
509 images. Singh et al. [125] implemented modified mean-shift-based FCM segmentation for brain
510 tumor detection in MRI images. The results indicated a high level of efficiency and accuracy for
511 the suggested technique. Kim et al. [126] offered a strategy for reducing file sizes and brain tumor
512 discovery in MRI images using modified K-means and mean-shift clustering techniques. The
513 researchers reported that the proposed method reached a precision of 0.914052 and a recall of
514 0.995641.

515 The Mean-Shift clustering approach is able to define the number of clusters automatically and
516 no problem generated from outliers. However, this method unable to work well in case of changing
517 the number of clusters changes abruptly (high dimension).

518 *4.2.4 Hierarchical clustering*

519 Hierarchical clustering, also known as hierarchical cluster analysis, is an algorithm to categorize
520 similar objects in groups called clusters [127]. Hierarchical clustering includes a multilevel
521 hierarchy tree where clusters at one level are joined as clusters at the next level. The algorithm
522 clusters together object with similar attributes [128]. Finally, the algorithm returns a set of clusters
523 or groups, where clusters are different from each other and objects within clusters are similar to
524 each other. These algorithms have been applied in the medical domain for brain tumor clustering.
525 For instance, Hiratsuka et al. [129] examined samples of human brain tumors using imaging mass
526 spectrometry (IMS). IMS analysis was integrated with the Region Of Interest Analysis (IMS-ROI)
527 and a novel Hierarchical Cluster Analysis (IMS-HCA). IMS-HCA and IMS-ROI appear to be
528 promising methods for finding biomarkers in brain cancer samples, according to the study's
529 findings. Tamilmani & Sivakumari [130] proposed a novel Association Allotment Hierarchical
530 Clustering (AAHC) approach for early brain cancer detection. The final results revealed that the
531 suggested approach reached an accuracy of 100%, outperforming the state-of-the-art method.
532 Moreover, the method was proven to be more computationally efficient compared to other models.

533 The Hierarchical clustering approach is able to define the number of clusters. However, this
534 method unable to work well with huge datasets or vast amounts of data.

535 *4.2.5 DBSCAN*

536 DBSCAN or Density-Based Spatial Clustering of Applications with Noise is a state-of-the-art
537 algorithm based on density [131]. The prominent feature of this algorithm is detecting clusters in
538 all sizes and shapes in different databases, even those with noise and outliers [132]. This approach
539 was employed to diagnose brain tumors. For instance, Muthaiyan et al. [133] proposed systems to
540 discover brain tumors using images taken using MRI and PET by different classification methods,
541 such as Gustafson-Kessel (G-K) algorithm, k-means clustering algorithm, DBSCAN, and FCM.
542 The effectiveness of various algorithms is compared, and DBSCAN is not among the most

543 effective methods for detecting brain cancer. Moreover, Bandyopadhyay [134] used DBSCAN and
 544 K-means clustering for the problem of segmenting and grouping brain tumors from MRI images
 545 of the human brain, and the result of the study indicated the effectiveness of the DBSCAN
 546 approach in comparison with the K-means technique.
 547 The DBSCAN clustering approach not only is able to define the number of clusters but also is able
 548 to find arbitrarily shaped and size of clusters. However, this method fails in case of varying density
 549 clusters.

550 4.2.6 Gaussian Mixture Models

551 As a probabilistic model, GMM presumes that a combination of a limited number of Gaussian
 552 distributions, which have unknown parameters, generate all the data points [135]. To investigate
 553 the effectiveness of GMM in brain cancer segmentation, Chaddad [136] introduced a unique
 554 technique for extracting Glioblastoma (GBM) features from MRI data using GMM. The accuracy
 555 performance for the T1-WI and T2-WI was 97.05% and 97.05%, respectively. The accuracy
 556 dropped to 94.11 % in FLAIR mode. These experimental findings show promise for improving
 557 heterogeneity features and, consequently, early GBM treatment. Pravitasari et al. [137] segmented
 558 the MRI-based brain tumor utilizing the GMM and the Reversible Jump Markov Chain Monte
 559 Carlo algorithm. The study's findings showed that the suggested technique executed the algorithm
 560 quickly and efficiently.

561 The GMM approach is less sensitive to the number of parameters. However, this method has a
 562 slow convergence rate and is sensitive to initialization values.

563 4.3 Overview of Supervised and Unsupervised Methods Application

564 Table 6 displays the 12 papers that applied either supervised or unsupervised approaches. It
 565 should be mentioned that all these papers are selected randomly. According to this table, as most
 566 of the researchers applied the BRaTS dataset, MRI image modalities are T1, T1c, T2, and FLAIR.
 567 The advantages of each approach are mentioned in the last column.
 568

569 **Table 6.** Overview of recent segmentation methods.

Author	Method of Segmentation	MRI Modalities	Dataset	Advantage
Bonte et al.[138]	Random Forest	T1ce and FLAIR MRI	BRaTS 2013 database	1. Requires fresh training sets. 2. Very much sensitive to noise
Bahadure et al. [139]	watershed	-	15 images with 9 slices using 3 Tesla Siemens Magnetom Spectra MR machine	1. Sensitivity to intensity variants. 2. Ignore the blurry boundaries. 3. High system complexity.
	FCM			
	DCT			
	BWT			

Author	Method of Segmentation	MRI Modalities	Dataset	Advantage
Reddy & Reddy. [140]	Region growing algorithm	T1, T1c, T2, and FLAIR	BRATS 2015	1. Over segmentation. 2. Need seed point selection.
Xie & Xiaozhen. [141]	KNN	T1 and T2	-	1. Poor run-time performance. 2. Only using T1 and T2 modalities.
Raja & Rani. [142]	Bayesian fuzzy clustering	T1, T1c, T2, and FLAIR	BRATS 2015	1. High system complexity. 2. Time-consuming.
Ilhan & Ilhan. [143]	Novel Threshold-based method	Flair, T2 and T1C	TCIA: 100 MRI images	1. Poor run-time performance. 2. High system complexity
Aslamet al. [144]	Sobol Edge-detection	-	-	1. Not acceptable result at fuzzy borders. 2. Not clear the process of the model.
Kermi et al. [145]	region-based + boundary-based	T1, T1ce, T2, and Flair	BRaTS'2017	1. Poor run-time performance
Sheela & Suganthi. [146]	Region of Interest + Region Growing + Morphological Operation	-	medical MR Images of 120 patient	1. High system complexity. 2. Class imbalances not considered.
Khan et al. [147]	k-means+ VGG19	T1, T1c, T2, and FLAIR	BRaTS 2015	1. Many features are required. 2. Easy to lose information
ŞİŞİK & SERT. [148]	BTS-ELM-FRFCM	T1	3200 pieces MRI image	1. Only using T1 modality. 2. Class imbalances not considered.
Khosravanian et al. [149]	superpixel fuzzy clustering +lattice Boltzmann	T1, T1ce, T2, and Flair	BRaTS 2017	1. Ignore the blurry boundaries. 2. High system complexity

570

571

572

573

574

575

576

577

578

579

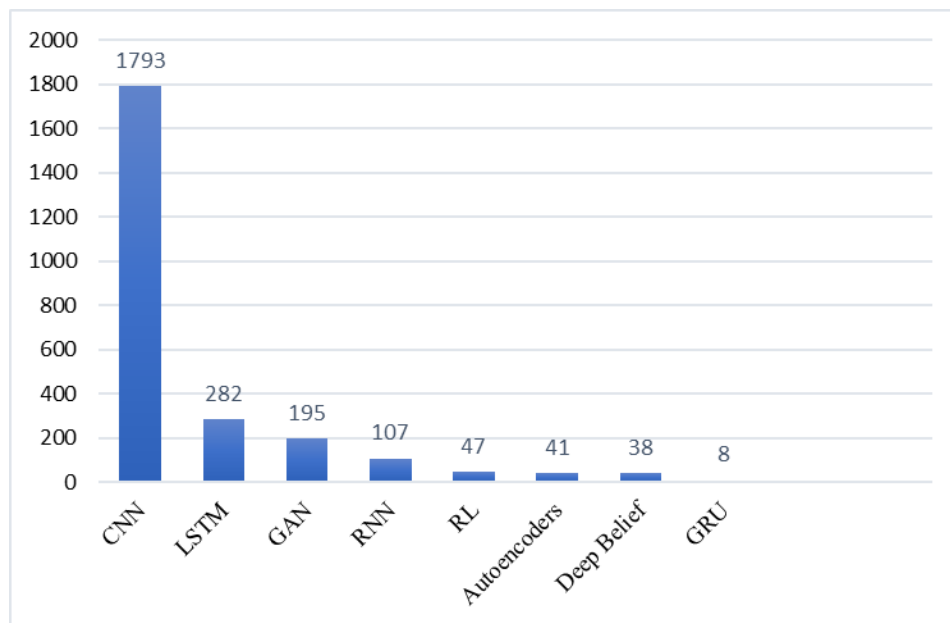
580

5. Deep Learning Application in Brain Tumor Segmentation

DL is a form of ML and AI that mimics how humans gain specific subjects. In data science, which also encompasses statistics and predictive modeling, DL plays a significant role. Multiple visual analysis tasks, including classification, object detection, and tracking, have provided notable performance gains due to DL techniques [150]–[154]. Additionally, DL techniques have had a significant impact on the automation of medical image processing tasks while showing state-of-the-art accuracy. Over the last decades, many DL techniques have been developed and applied in different areas, including brain tumor diagnosis [155]. In the following, the popular DL approaches that are utilized for brain cancer diagnosis are introduced. Fig. 5 illustrates the number of papers

581 that applied different approaches of DL to investigate their performance in brain cancer
582 segmentation and classification. According to the Fig. 5, the number of studies that applied CNN-
583 based approaches is considerably higher than other DL approaches with 1793 publications between
584 2015 to 2022. LSTM is the second DL approach that has been employed in brain tumor diagnosis
585 with 282 papers.

586



587 **Fig. 5.** Number of publications between 2015 to 2022 for brain tumor segmentation using DL models.

588

589

590

5.1 Convolutional Neural Network

591 A Convolutional Neural Network (CNN), or ConvNet, sets the basis for DL [156], [157]. In
592 this method, learning is received straight from the data, so there is no need to extract features
593 manually [51]. The most significant usage of CNNs is in discovering patterns in images [158]. A
594 CNN network can be trained using a large dataset from scratch by fine-tuning an existing model
595 or utilizing "off-the-shelf CNN features" [152]. Fine-tuning involves transferring weights of the
596 first n layers learned from an earlier-based network to the new network [159]. The dataset obtained
597 for the new network is trained to perform specific tasks. By effectively learning general image
598 features through transfer learning, CNNs are able to tackle the majority of computer vision
599 problems by combining these features with straightforward classifiers [50]. This is the main reason
600 why the CNN approach has been applied considerably for brain tumor diagnosis. For example,
601 Abd El Kader et al. [160] used deep differential CNN to categorize brain tumors in MRI images.
602 This method achieved maximum accuracy of 99.25%.

603 Bacanin et al. [161] deployed the firefly algorithm to optimize CNN for glioma brain tumor
604 grade classification. The researchers reported that the introduced method reached the maximum
605 multi-class accuracy of 97.9% and the maximum accuracy of 96.5% in the images containing brain
606 tumors. Wang et al. [162] offered a ground-breaking structure based on CNN with a dilated

607 convolutional feature pyramid called DFP-ResUNet to categorize multimodal brain tumors. The
608 results of testing the suggested model on the BRaTS 2018 dataset showed the mean Dice value of
609 different subregions to be Enhancing Tumor (ET) 0.8431, Whole Tumor (WT) 0.897, and Tumor
610 Core (TC) 0.9068. Gurunathan and Krishnan [163] applied CNN for brain tumor detection and
611 diagnosis using MRI images. The method reached the maximum classification accuracy of 98.3%,
612 the sensitivity of 97.2%, and the specificity of 98.9%.

613 The CNN models are able to explore hidden patterns inside the input data automatically and
614 share weights between layers. However, these models fail to encode the orientation and position
615 of objects.

616

617 **5.2 Recurrent Neural Network**

618 As an ANN, a Recurrent Neural Network (RNN) employs time series data or sequential data
619 [164]. RNNs have the concept of "memory," which enables the method to retain the qualities or
620 details of the former inputs in order to produce the following output in the sequence. RNNs are
621 characterized by their capacity to transmit data over time steps [165]. RNNs feature an extra
622 parameter matrix in their structure for connections between time steps, which encourages training
623 in the temporal domain and makes use of the input's sequential nature. In the RNN technique, the
624 predictions made at each time step are trained to be based on both the most recent input and data
625 from earlier time steps [166]. RNNs hold the second place of the most favored approaches to
626 diagnose brain cancer and have been implemented in many studies. For example, SivaSai et al.
627 [167] used fuzzy RNN to categorize brain tumors in MRI images automatically. The results
628 showed an accuracy of 87.8% and it was proven that the proposed framework is much more
629 computationally efficient. Zhou et al. [168] deployed DenseNet and RNN for a holistic screening
630 and categorization of brain tumors via MRI images. By testing the proposed structure on public
631 datasets, the researchers reported that the DenseNet-RNN approach reached the maximum
632 accuracy of 84.61%. However, DenseNet-LSTM achieved an accuracy of 92.13% and performed
633 better than RNN based approach. Begum and Lakshmi [169] combined optimal wavelet statistical
634 texture and RNN to discover and classify brain tumors in MRI images. The proposed method
635 achieved a maximum accuracy of 96% and a maximum sensitivity of 100% in the classification.
636 Moreover, the introduced approach reached the maximum accuracy and sensitivity of 95% and
637 97%, respectively for the segmentation.

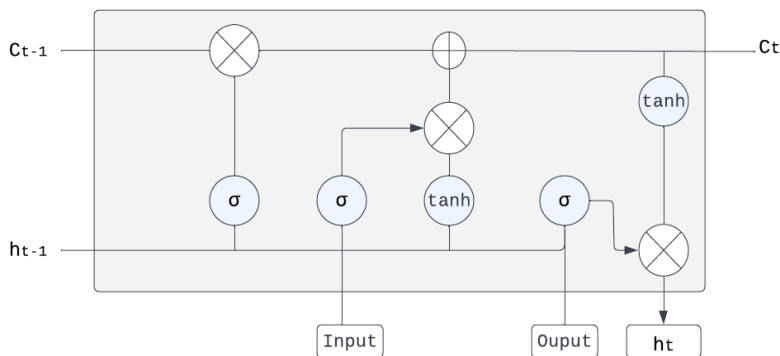
638 The RNN models are capable of processing inputs of any length and each sample can be
639 assumed to be dependent on former samples. However, these models face issues like Vanishing
640 Gradient or Exploding Gradient.

641

642 **5.3 Long Short-Term Memory**

643 There are recurring neural networks able to learn order dependency in issues related to
644 predicting sequences; these networks are called Long Short-Term Memory (LSTM) networks
645 [170]. LSTM is one of the most widely-used RNN designs to date. It is the best option for modeling

646 sequential data and is thus utilized to learn the complex dynamics of human behavior. The word
 647 "cell state" refers to long-term memory. Previous data is stored in the cells because of their
 648 recursive nature. LSTM was specifically created and developed in order to address the
 649 disappearing gradient and exploding gradient issues in long-term training [171]. Fig. 6 shows an
 650 example of LSTM structure and the way this technique works.



651
 652 **Fig. 6.** An example of LSTM structure.
 653

654 This approach has been utilized in previous studies to diagnose a brain tumor. For example,
 655 Dandil and Karaca [172] used stacked LSTM for pseudo brain tumor detection based on MRI
 656 spectroscopy signals. The experimental results indicated an accuracy of 93.44% for the
 657 categorization of pseudo brain tumor with glioblastoma, 85.56% accuracy for a pseudo brain tumor
 658 with diffuse, 88.33% for a pseudo brain tumor with astrocytoma, and 99.23% for a pseudo brain
 659 tumor with metastatic brain tumors. Xu et al. [173] proposed an LSTM Multi-modal UNet to
 660 categorize tumors using multi-modal MRI. The experimental results by testing the model's
 661 performance on the BRATS-2015 dataset showed that the proposed LSTM multi-modal UNet
 662 outperformed the standard U-Net with fewer model parameters. Shahzadi et al. [174] developed an
 663 approach according to a cascade of CNN with an LSTM network for 3D brain tumor MR image
 664 classification. The researchers reported an accuracy of 84% for the proposed method.

665 The LSTM models are capable of learning long-term dependencies. However, these models
 666 prone to overfitting and need a lot of resources, high memory-bandwidth, and time to get trained.
 667

668 **5.4 Generative Adversarial Network**

669 Generative Adversarial Network (GAN) is one of the categories of generative models [175].
 670 These models have the capacity to create or develop new data with the statistics similar to the
 671 training set given. For instance, a GAN trained on images can produce new images with numerous
 672 realistic features that appear to be created by humans, at least on the surface [176]. Fig. 7 indicates
 673 the simple structure of the GAN approach.

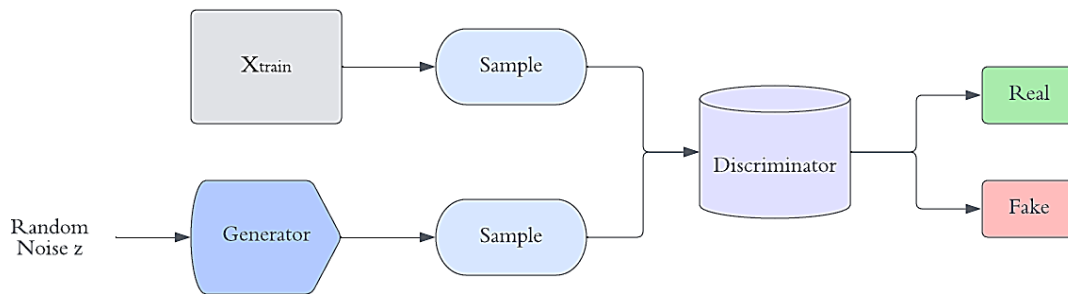


Fig. 7. An example of the GAN method structure.

674
675
676

677 In order to evaluate the efficiency of the GAN method in segmenting brain tumors, several
678 studies have been conducted. For example, Nema et al. [177] developed a novel architecture called
679 residual cyclic unpaired encoder-decoder network (RescueNet) to segment brain tumors which is
680 trained based on an unpaired GAN. The results showed a Dice value of 0.9401% and 0.9463% for
681 the BRaTS 2015 and BRaTS 2017 datasets, respectively. Neelima et al. [178] provided an
682 approach founded on the Optimal DeepMRSeg strategy trained by a devised Sailfish Political
683 Optimizer (SPO) algorithm to segment the tumors and then applied GAN to classify brain tumors
684 using MRI images. The elevated accuracy, segmentation accuracy, sensitivity, and specificity
685 resulted from this method were 91.7%, 90%, 92.8%, and 92.5%, respectively. Rezaei et al. [179]
686 proposed a new method according to the adversarial network called voxel-GAN for mitigating
687 imbalanced data problems in segmenting the tumors using 3D brain MR or CT images. Once the
688 suggested method was evaluated on the ISLES dataset, the results showed a Dice value of 0.83, a
689 Hausdorff score of 9.3, a precision of 0.81, and a recall of 0.78.

690 The LSTM models are capable of improving data instances, lowering costs, and increasing
691 data production. However, these models require strong technical knowledge and advanced
692 datasets.

693

694 **5.5 Deep Belief Network**

695 Deep Belief Networks (DBNs) are a type of graphical representation that is fundamentally
696 generative, producing all possible values for the given case. It combines ML and neural networks
697 with probability and statistics [180]. DBNs are made up of many layers with values, but there is
698 no relationship between the values and the layers. The major objective is to assist the system in
699 categorizing the data into distinct categories. Fig. 8 represents a simple structure of the DBN
700 approach.

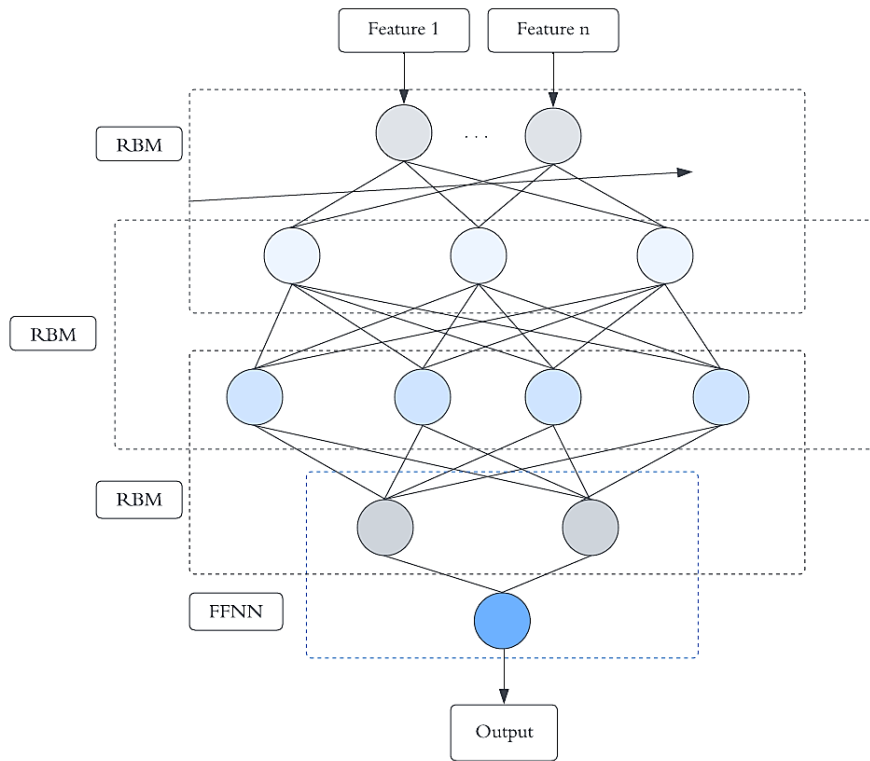


Fig. 8. An example of DBN method structure.

701
702
703

704 In other cancer studies, it is indicated that DBN is among the best approaches to segment
705 tumors. There are several research works that used DBN for brain tumor segmentation. For
706 example, Kharrat and Néji [181] implemented personalized DBNs for brain tumor classification
707 using MRI images. The researchers trained the proposed model on the BRaTS dataset and showed
708 the model reached an accuracy of 91.6%. Raju et al. [182] offered a strategy according to a DBN
709 and hybrid active contour model to split and classify the tumors of the brain via MRI images. The
710 outcomes indicated the accuracy of 0.945, sensitivity of 0.9695, and specificity of 0.99348 for the
711 proposed model.

712 The DBN models are capable of providing the best performance results even if the amount of
713 data is huge. However, these models require strong technical knowledge and huge data to perform
714 better.

715
716

5.6 Autoencoders

717 Autoencoders are an unsupervised learning method that uses neural networks for the
718 presentation learning task [183]. Specifically, it is a neural network architecture with an imposed
719 bottleneck that represents a compact knowledge of the specified input [184]. Amin et al. [185]
720 deployed Stacked Sparse AutoEncoders (SSAE) to detect brain tumors. They tested the suggested
721 model on the BRaTS datasets and reached the average accuracies of 100%, 90%, 95%, 100%,
722 97%, and 95% on the 2012 dataset, 2012 synthetic dataset, 2013 dataset, Leaderboard 2013 dataset,

723 2014 and 2015 datasets, respectively. Badža and Barjaktarović [186] implemented a convolutional
724 autoencoder to segment brain tumors based on MRI images. The researchers reported that the
725 proposed method achieved 99.23% average accuracy for pixel classification and an average
726 accuracy of 99.28% for 5-fold cross-validation and one test.

727 The Autoencoders can reduce the dimensionality of the data, provide an appropriate way to
728 diminish the noise of input data greatly, and make the creation of DL frameworks much more
729 efficient. However, learning and reproducing input features in training autoencoders is unique to
730 the data they are trained on and don't work for new data.

731

732 **5.7 Reinforcement Learning**

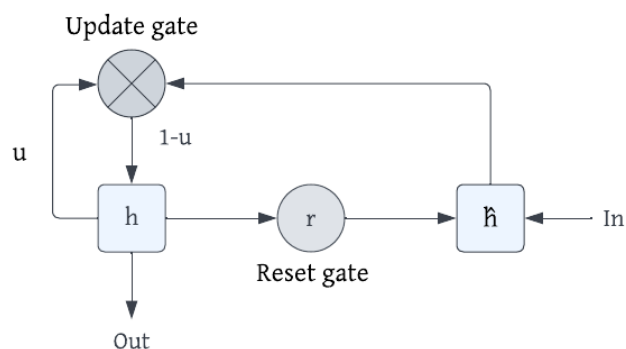
733 Reinforcement Learning (RL) is the training of ML models to make a sequence of decisions.
734 The agent gains the ability to do a task in a possibly complex and uncertain environment. An AI
735 encounters a scenario similar to a game during RL. In order to solve the problem, the computer
736 uses trial and error. AI is rewarded or punished for the steps it takes to make the machine do what
737 the programmer desires. The goal of the RL algorithm is to maximize the total reward Stember
738 and Shalu [187] automatically extracted labels from clinical reports and then utilized deep RL
739 classifier to classify 3D MRI brain volumes. The results revealed that the presented method
740 provides 100% accuracy.

741 The RL models are desired to gain long-term outcomes, which are challenging to obtain.
742 Moreover, a perfect model can be created to solve a particular problem. However, RL models need
743 plenty of data and computation and are not preferable to utilize for solving simple problems.

744

745 **5.8 Gate Recurrent Unit**

746 Gated Recurrent Unit (GRU) is the upgraded version of the standard RNN, i.e. RNN, which
747 was offered by Kyunghyun Cho et al. [188] GRUs are very similar to Long Short Term Memory
748 (LSTM). Resembling the LSTM, GRU employs gates to supervise the flow of information, which
749 are newer than LSTM. Therefore, they improve LSTM and focus on simplifying the architecture.
750 Fig. 9 displays the structure of the GRU model.



751

752

Fig. 9. An example of GRU method structure.

753

754 One of the main usages of the GRU is increasing the memory capacity of a RNN and facilitating
 755 the training of a model. On top of that, we can employ the hidden unit and solve the problem of
 756 vanishing gradients in RNNs. There are investigations that applied the GRU technique for brain
 757 cancer diagnosis. For example, Gab Allah et al. [189] employed a combination of a VGG-16
 758 network and a GRU model to increase the brain tumor segmentation in the presence of even fuzzy
 759 borders. Table 7 indicates the 16 papers that used DL approaches to classify and segment brain
 760 tumors.

761 Unlike LSTM, GRU models do not have a separate cell state (Ct) and only have a hidden state
 762 (Ht). These models are much faster due to the simpler architecture.

763

764

Table 7. Overview of segmentation through DL approaches.

Author	Method of Segmentation	MRI Modalities	Dataset	Limitations
Chang et al. [190]	CNN+FCRE	T1, T2, T1c, FLAIR	BRaTS2013	1. Requires fresh training sets. 2. Only using HGG patient subjects.
Kaldera et al. [191]	Faster R-CNN	T1	MRI dataset of Nanfang Hospital and General Hospital in China	1. Requires fresh training sets. 2. Only using T1 modality.
Sajjad et al [192]	CNN + Data augmentation	T1	Radiopaedia dataset	1. Need a post-processing step. 2. Only using T1 modality.
Murthy et al [193]	Optimized CNN	-	kaggle	1. Requires fresh training sets. 2. Need a post-processing step.
Rehman et al [194]	3D CNN	T1, T2, T1c, FLAIR	BRaTS 2015, 2017, and 2018	1. Fail to detect the unobvious and small brain tumors. 2. High system complexity
Amin et al [195]	LSTM	T1, T2, T1c, FLAIR	BRaTS +SISS database	1. High system complexity. 2. Requires fine-tuning of the network parameters.
Liu et al [196]	DRL + DTCWT	T1, T2, T1c, FLAIR	BRaTS2018 + CQ500 + hospital databases	1. High system complexity 2. Lack of spatial consistency.
Kumar et al [197]	DBN + GS-MVO	T1	Kaggle dataset	1. The feature selection is not clear. 2. Only using T1 modality.

Author	Method of Segmentation	MRI Modalities	Dataset	Limitations
Harish & Baskar [198]	R-CNN + Alex Net model	-	-	1. Many layers, which increases system complexity. 2. Requires fresh training sets.
Ahmad et al. [199]	Variational Autoencoders + GAN	T1	Figshare	1. Requires fine-tuning of the network parameters 2. Only using T1 modality.
Mukherkjee et al. [200]	Optimized GAN method	T1, T2, T1c, FLAIR	BRaTS 2020 dataset	1. High computational cost. 2. High system complexity.
Takrouni & Douik [201]	DPGM+DDM	T1, T2, T2c & FLAIR	BRaTS 2013 + 2015 +2017	1. Need a lot of training data. 2. High system complexity.
Chattopadhyay & Maitra [202]	CNN	T1, T2, T2c & FLAIR	BRaTS 2020	1. Weak interpretability. 2. Requires fresh training sets.
Kesav & Jibukumar [203]	RCNN	T1	Figshare + Kaggle	1. Requires fine tuning of the network parameters 2. Only using T1 modality.
Vankdothu et al [204]	CNN + LSTM	T1	Kaggle	1. High system complexity. 2. Only using T1 modality.
Ranjbarzadeh et al. [18]	CNN + Attention	T1, T2, T2c & FLAIR	BRaTS 2018	1. High system complexity. 2. Requires fresh training sets.

765

766

6. Brain Tumor Imaging Database

767

768

769

770

771

There are many advanced databases of medical images taken from patients suffering from brain tumors to facilitate the development and validation of new images. Table 8 outlines the list of top brain databases used in recent investigations. The number of data and their modalities mentioned.

Table 8. Top database for the brain tumors.

Dataset	From	Number of images	Available Modalities
BRATS 2012	MICCAI 2012 Challenge	45 3D	T1, T2, T1c, FLAIR
BRATS 2013	MICCAI 2013 Challenge	65 3D	T1, T2, T1c, FLAIR
BRATS 2014	MICCAI 2014 Challenge	50 3D	T1, T2, T1c, FLAIR
BRATS 2015	MICCAI 2015 Challenge	300 3D	T1, T2, T1c, FLAIR
BRATS 2016	MICCAI 2016 Challenge	300 3D	T1, T2, T1c, FLAIR
BRATS 2017	MICCAI 2017 Challenge	285 3D	T1, T2, T1c, FLAIR
BRATS 2018	MICCAI 2018 Challenge	285 3D	T1, T2, T1c, FLAIR
BRATS 2019	MICCAI 2019 Challenge	335 3D	T1, T2, T1c, FLAIR
BRATS 2020	MICCAI 2020 Challenge	-	T1, T2, T1c, FLAIR

Dataset	From	Number of images	Available Modalities
BRATS 2021	MICCAI 2021 Challenge	-	T1, T2, T1c, FLAIR
ADNI1	Alzheimer's disease neuroimaging initiative	400	T2, FLAIR, DTI
BrainnWeb	McConnell Brain Imaging Centre	21	T1, T2, PD- weighted
RIDER	TCIA	365 3D	T1, T2- weighted
AANLIB	Harvard Medical School	-	T1, T2- weighted MRI
The IBSR	The CMA	39	T1- weighted
Allen brain atlas	Allen Institute Publications for Brain Science	20	T1, T2, DTI
Figshare	Jun Change	3064	T1
Kaggle	-	3264	-
SISS	-	-	FLAIR, DWI, T2, T1

772

773 6.1 BRaTS Database

774 According to Table 8, BRaTS are the most used data set for brain cancer diagnosis. BRaTS
775 database employs special MRI scans that are multi-institutional and pre-operative to concentrate
776 on parting incongruous brain tumors, i.e., gliomas, which are different in appearance, shape, and
777 histology. Table 9 indicates the dice and Hausdorff parameter for the papers that applied the
778 different methods to diagnose brain tumors based on BRaTS database.

779

780

Table 9. Dice and Hausdorff index of investigations based on BRaTS 2020-2017.

BRaTS 2020						
Method	Dice			Hausdorff 95%		
	Comp	Core	Enh	Comp	Core	Enh
3D U-Net [205]	89%	84%	81%	6.4	19.4	15.8
nnU-Net [206]	89%	85%	82%	8.50	17.33	17.80
Multiple U-net [207]	89%	84%	78%	6.7	19.55	20.4
Scale Attention Network [208]	88%	84%	82%	5.2	17.97	13.43
Variational-autoencoder + regularized 3D U-Net [209]	89%	79%	70%	4.62	10.07	34.30
Deep Layer Aggregation [210]	88%	83%	79%	5.32	22.32	20.44
Lightweight U-Nets [211]	87%	80%	75%	6.2	19.6	21.46
HI-Net [212]	88%	84%	79%	-	-	-
Modified UNet [213]	89%	85%	79%	-	-	-
DR-Unet104 [214]	87%	80%	75%	10.41	21.84	24.68
BRaTS 2019						
Method	Dice			Precision		

	Comp	Core	Enh	Comp	Core	Enh
Two-stage Cascade UNet [215]	89%	84%	83%	4.62	4.13	2.65
Encoder-decoder + Combined loss function [216]	88%	84%	83%	4.7	3.97	2.20
CNN [217]	87%	78%	78%	7.3	6.8	3.7
3D UNet [218]	85%	80%	78%	6.5	6.3	3.5
RMU-Net [219]	92%	91%	83%	-	-	-
Deep Layer Aggregation [220]	87%	83%	79%	5.32	22.32	20.44
DNN [221]	88%	86%	81%	4.8	5.6	2.4
Multi-Resolution 3D CNN [222]	82%	72%	70%	8.42	9.14	5.59
3D Residual U-Net [223]	83%	77%	70%	14.64	26.69	25.56
3D FCN [224]	89%	78%	76%	-	-	-
BRaTS 2018						
	Dice			Precision		
Method	Comp	Core	Enh	Comp	Core	Enh
3D UNet [225]	86%	82%	76%	7.01	5.63	5.6
Deep CNN [226]	88%	79%	78%	5.5	6.9	2.93
3D UNet [227]	87%	77%	71%	6.5	8.31	4.14
Contour-aware 3D CNN [228]	89%	79%	72%	8.05	7.5	5.2
S3D-UNet [229]	84%	78%	69%	9.2	7.7	4.5
HTTU-Net [230]	88%	89%	82%	7.53	8.81	4.43
Auto-encoder Regularization [231]	88%	81%	77%	5.9	4.8	3.8
Cascaded UNet [232]	88%	78%	72%	-	-	-
CNN [233]	87%	77%	78%	6.55	27.05	15.90
CNN + Test-time Augmentation [234]	88%	80%	75%	5.97	6.71	4.16
BRaTS 2017						
	Dice			Precision		
Method	Comp	Core	Enh	Comp	Core	Enh
UNet [235]	81%	76%	65%	-	-	-
Random Forest +CNN [236]	85%	69%	67%	6.12	28.72	23.55
FCN [237]	70%	55%	40%	-	-	-
Anisotropic CNN [238]	87%	77%	78%	6.5	27	15.90
EMMA [239]	89%	80%	73%	5.01	23.1	36.0
CNN [240]	83%	65%	65%	-	-	-
UNet [241]	88%	76%	64%	-	-	-
Pixel Net [242]	87%	76%	68%	9.8	12.30	12.93
Multi-path CNN [243]	84%	69%	60%	-	-	-

781

782 **7. Performance measures**

783 The performance assessment of the classification or segmentation strategies can be
 784 accomplished using different methods. Researchers employ various strategies for validating the
 785 obtained outcomes. The most popular and widely used performance measures
 786 including Sensitivity (Recall or True Positive Rate), Specificity, Accuracy, and Precision,
 787 Confusion matrix, Jaccard Index, and Dice Similarity. These criteria can be defined as follows:

788 Confusion matrix (CM) is used to provide crucial information about actual and estimated
 789 outcomes created by the classification or segmentation techniques. One example of a two-class
 790 classification task is demonstrated as in Table 10.

791

792

Table 10. The details of classification criteria for two classes.

Category	Estimated Brain tumor	Ordinary tissue
Brain tumor	True Positive (TP)	False Negative (FN)
Ordinary tissue	False positive (FP)	True Negative (TN)

793

794 Where TP,FP, FN, and TN are described as:

795 TP: Correctly classified or segmented brain tumor.

796 TN: Correct classified or segmented of Ordinary tissue as Ordinary tissue.

797 FN: Wrong classified or segmented of actual tumor tissue as Ordinary tissue.

798 FP: Wrong classified or segmented of an ordinary tissue.

799

$$Accuracy = \left(\frac{TN + TP}{TN + TP + FP + FN} \right) \quad (1)$$

$$DICE = \left(\frac{2 \times TP}{(2 \times TP) + FP + FN} \right) \quad (2)$$

$$Precision = \left(\frac{TP}{TP + FP} \right) \quad (3)$$

$$Specificity = \left(\frac{TN}{TN + FN} \right) \quad (4)$$

$$Sensitivity \text{ or Recall} = \left(\frac{TP}{TP + FN} \right) \quad (5)$$

$$Jaccard \text{ Index } (A, B) = \frac{|A \cap B|}{|A \cup B|} \quad (6)$$

800

801 **8. Discussion**

802 The brain tumor is one of the fatal diseases that occurs when the growth of cells in the brain is
803 out of control. The mortality rate of this cancer made researchers investigate approaches for early
804 brain cancer diagnosis. MRI images are one of the best tools to diagnose cancer by providing a
805 picture of soft tissue in the brain. Over the last decades, many ML-based and DL-based approaches
806 have been developed. However, due to the large number of articles that implemented these
807 approaches, it is important to summarize the current studies and methods. In this work, we provide
808 a holistic approach and summarize ML-based segmentation approaches, DL-based segmentation
809 methods, a review of top DL and ML papers, the top database of brain cancer, and a comparison
810 of accuracy rate in applying different methods on publicly available datasets. The application of
811 CAD systems that work based on DL and ML approaches in brain tumor diagnosis increases
812 accuracy, decreases failure in diagnosis, early detection, and provides better treatment approaches.
813 Also, in underdeveloped countries with a scarcity of experts, CAD-based systems can provide
814 early diagnosis, which results in a decrease in mortality rate.

815 The analyses of the previous studies indicated that MRI is the best imaging technique for brain
816 tumor diagnosis (Tables 6 and 7). The main reason for the widespread usage of MRI is that this
817 imaging technique provides more details compared to other approaches like CT scans. Moreover,
818 over the last years, the application of DL approaches was significantly more than ML techniques.
819 According to Figs. 4 and 5, the number of total papers that applied DL approaches has increased
820 significantly. However, the number of papers that implemented ML techniques or hybrid methods
821 is still more than DL-based approaches. SVM and CNN are the most used ML and DL approaches
822 for brain tumor segmentation. Moreover, in most papers, BRaTS datasets are employed. According
823 to Table 9, the dice and Hausdorff rate indicate that the BRaTS dataset can also be used in future
824 studies as they are reliable.

825

826 **9. Conclusion**

827 Brain tumor segmentation has widely benefitted from advancements in AI. Researchers have
828 been applying AI algorithms and techniques for detecting brain tumors, computing tissue volumes,
829 abnormality detection, pathology, planning of treatments, and computer-aided surgery. These
830 techniques work well in tasks related to segmenting brain tumors as their features enable
831 distinguishing abnormal tissues from normal ones. This paper offers a general survey of methods
832 applied to brain tumor segmentation. A long array of automatic and semi-automatic brain tumor
833 segmentation, classification, and feature extraction methods is covered in this study. The current
834 paper quantitatively measures the up-to-date approaches based on multiple evaluation metrics to
835 help readers and medical experts both to develop future research directions and, more importantly,
836 identify the most effective and precise strategies to segment tumors of the brain. This paper
837 proposes that the upcoming research aiming to enhance the performance of the current systems for
838 brain segmentation can be followed in several directions: (i) Gathering larger databases with

839 images from various qualities, (ii) Focusing on improving the classification accuracy of current
840 methods by developing novel methods for feature extraction, and (iii) Developing hybrid systems
841 consisting of multiple approaches regarding ML and DL.

842 Except the techniques employed in this study, some of the most representative computational
843 intelligence techniques can be utilized to solve the problems, like Harris hawks optimization
844 (HHO), Monarch Butterfly Optimization (MBO), Earthworm Optimization Algorithm (EWA),
845 Moth Search Algorithm (MSA), Colony Predation Algorithm (CPA), Slime Mould Algorithm
846 (SMA), Hunger Games Search (HGS), and Runge Kutta Optimizer (RUN).

847 However, it is still questionable whether the abundance of computational resources, deep learning
848 technology, and training data needed to run DL at full performance is meaningful, considering
849 other learning techniques that may yield fast, higher interpretability, and close performance with
850 less parameterization, tuning, and fewer resources.

851

852 **Acknowledgement**

853 This publication has emanated from research [conducted with the financial support of/supported
854 in part by a grant from Science Foundation Ireland under Grant number No. 18/CRT/6183 and is
855 supported by the ADAPT Centre for Digital Content Technology which is funded under the SFI
856 Research Centres Programme (Grant 13/RC/2106/_P2), Lero SFI Centre for Software (Grant
857 13/RC/2094/_P2) and is co-funded under the European Regional Development Fund. For the
858 purpose of Open Access, the author has applied a CC BY public copyright license to any Author
859 Accepted Manuscript version arising from this submission.

860

861 **Declaration of interests**

862 The authors declare that they have no known competing financial interests or personal
863 relationships that could have appeared to influence the work reported in this paper.

864

865

866

867 **References**

868 [1] A. Petruzzi, C. Y. Finocchiaro, E. Lamperti, and A. Salmaggi, "Living with a brain tumor,"
869 *Supportive Care in Cancer* 2012 21:4, vol. 21, no. 4, pp. 1105–1111, Oct. 2012, doi:
870 10.1007/S00520-012-1632-3.

871 [2] C. Kruchko, Q. T. Ostrom, H. Gittleman, and J. S. Barnholtz-Sloan, "The CBTRUS story: providing
872 accurate population-based statistics on brain and other central nervous system tumors for everyone,"
873 *Neuro Oncol*, vol. 20, no. 3, pp. 295–298, Feb. 2018, doi: 10.1093/NEUONC/NOY006.

- 874 [3] A. Tahir, M. Asif, M. Bin Ahmad, T. Mahmood, M. A. Khan, and M. Ali, "Brain Tumor Detection
875 using Decision-Based Fusion Empowered with Fuzzy Logic," *Math Probl Eng*, vol. 2022, pp. 1–
876 13, Aug. 2022, doi: 10.1155/2022/2710285.
- 877 [4] K. D. Miller *et al.*, "Brain and other central nervous system tumor statistics, 2021," *CA Cancer J*
878 *Clin*, vol. 71, no. 5, pp. 381–406, Sep. 2021, doi: 10.3322/CAAC.21693.
- 879 [5] J. B. Iorgulescu *et al.*, "Molecular biomarker-defined brain tumors: Epidemiology, validity, and
880 completeness in the United States," *Neuro Oncol*, Apr. 2022, doi: 10.1093/NEUONC/NOAC113.
- 881 [6] P. A. McKinney, "Brain tumours: incidence, survival, and aetiology," *J Neurol Neurosurg*
882 *Psychiatry*, vol. 75, no. suppl 2, pp. ii12–ii17, Jun. 2004, doi: 10.1136/JNNP.2004.040741.
- 883 [7] F. Özyurt, E. Sert, and D. Avci, "An expert system for brain tumor detection: Fuzzy C-means with
884 super resolution and convolutional neural network with extreme learning machine," *Med*
885 *Hypotheses*, vol. 134, p. 109433, Jan. 2020, doi: 10.1016/J.MEHY.2019.109433.
- 886 [8] N. Tataei Sarshar *et al.*, "Glioma Brain Tumor Segmentation in Four MRI Modalities Using
887 a Convolutional Neural Network and Based on a Transfer Learning Method," pp. 386–402, 2023,
888 doi: 10.1007/978-3-031-04435-9_39.
- 889 [9] N. A. Charles, E. C. Holland, R. Gilbertson, R. Glass, and H. Kettenmann, "The brain tumor
890 microenvironment," *Glia*, vol. 59, no. 8, pp. 1169–1180, Aug. 2011, doi: 10.1002/GLIA.21136.
- 891 [10] B. Cacho-Díaz, D. R. García-Botello, T. Wegman-Ostrosky, G. Reyes-Soto, E. Ortiz-Sánchez, and
892 L. A. Herrera-Montalvo, "Tumor microenvironment differences between primary tumor and brain
893 metastases," *Journal of Translational Medicine 2020 18:1*, vol. 18, no. 1, pp. 1–12, Jan. 2020, doi:
894 10.1186/S12967-019-02189-8.
- 895 [11] I. Koh and P. Kim, "In Vitro Reconstruction of Brain Tumor Microenvironment," *BioChip Journal*
896 *2019 13:1*, vol. 13, no. 1, pp. 1–7, Mar. 2019, doi: 10.1007/S13206-018-3102-6.
- 897 [12] J. Kotia, A. Kotwal, and R. Bharti, "Risk Susceptibility of Brain Tumor Classification to Adversarial
898 Attacks," *Advances in Intelligent Systems and Computing*, vol. 1061, pp. 181–187, 2020, doi:
899 10.1007/978-3-030-31964-9_17/COVER/.
- 900 [13] L. Desjardins *et al.*, "Predicting social withdrawal, anxiety and depression symptoms in pediatric
901 brain tumor survivors," <https://doi.org/10.1080/07347332.2018.1535531>, vol. 37, no. 1, pp. 22–36,
902 Jan. 2019, doi: 10.1080/07347332.2018.1535531.
- 903 [14] A. Wadhwa, A. Bhardwaj, and V. Singh Verma, "A review on brain tumor segmentation of MRI
904 images," *Magn Reson Imaging*, vol. 61, pp. 247–259, Sep. 2019, doi: 10.1016/J.MRI.2019.05.043.
- 905 [15] W. Zhang, Y. Wu, B. Yang, S. Hu, L. Wu, and S. Dhelimd, "Overview of Multi-Modal Brain Tumor
906 MR Image Segmentation," *Healthcare 2021, Vol. 9, Page 1051*, vol. 9, no. 8, p. 1051, Aug. 2021,
907 doi: 10.3390/HEALTHCARE9081051.
- 908 [16] P. K. Chahal, S. Pandey, and S. Goel, "A survey on brain tumor detection techniques for MR
909 images," *Multimedia Tools and Applications 2020 79:29*, vol. 79, no. 29, pp. 21771–21814, May
910 2020, doi: 10.1007/S11042-020-08898-3.
- 911 [17] W. L. Bi *et al.*, "Artificial intelligence in cancer imaging: Clinical challenges and applications," *CA*
912 *Cancer J Clin*, vol. 69, no. 2, pp. 127–157, Mar. 2019, doi: 10.3322/CAAC.21552.

- 913 [18] R. Ranjbarzadeh, A. Bagherian Kasgari, S. Jafarzadeh Ghoushchi, S. Anari, M. Naseri, and M.
914 Bendeche, "Brain tumor segmentation based on deep learning and an attention mechanism using
915 MRI multi-modalities brain images," *Sci Rep*, vol. 11, no. 1, p. 10930, Dec. 2021, doi:
916 10.1038/s41598-021-90428-8.
- 917 [19] M. Afridi, A. Jain, M. Aboian, and S. Payabvash, "Brain Tumor Imaging: Applications of Artificial
918 Intelligence," *Seminars in Ultrasound, CT and MRI*, vol. 43, no. 2, pp. 153–169, Apr. 2022, doi:
919 10.1053/J.SULT.2022.02.005.
- 920 [20] R. Singh, A. Goel, and D. K. Raghuvanshi, "Computer-aided diagnostic network for brain tumor
921 classification employing modulated Gabor filter banks," *The Visual Computer 2020 37:8*, vol. 37,
922 no. 8, pp. 2157–2171, Sep. 2020, doi: 10.1007/S00371-020-01977-4.
- 923 [21] A. Aghamohammadi, R. Ranjbarzadeh, F. Naiemi, M. Mogharrebi, S. Dorosti, and M. Bendeche,
924 "TPCNN: Two-path convolutional neural network for tumor and liver segmentation in CT images
925 using a novel encoding approach," *Expert Syst Appl*, vol. 183, p. 115406, Nov. 2021, doi:
926 10.1016/J.ESWA.2021.115406.
- 927 [22] R. Ranjbarzadeh and S. Baseri Saadi, "Corrigendum to 'Automated liver and tumor segmentation
928 based on concave and convex points using fuzzy c-means and mean shift clustering' [Measurement
929 150 (2020) 107086]," *Measurement*, vol. 151, p. 107230, Feb. 2020, doi:
930 10.1016/J.MEASUREMENT.2019.107230.
- 931 [23] S. B. Saadi *et al.*, "Osteolysis: A Literature Review of Basic Science and Potential Computer-Based
932 Image Processing Detection Methods," *Comput Intell Neurosci*, vol. 2021, 2021, doi:
933 10.1155/2021/4196241.
- 934 [24] J. Nalepa, M. Marcinkiewicz, and M. Kawulok, "Data Augmentation for Brain-Tumor
935 Segmentation: A Review," *Front Comput Neurosci*, vol. 13, p. 83, Dec. 2019, doi:
936 10.3389/FNCOM.2019.00083/BIBTEX.
- 937 [25] N. J. Shafana and A. Senthilselvi, "Analysis of AI based Brain Tumor Detection and Diagnosis,"
938 *Proceedings of the 2021 4th International Conference on Computing and Communications
939 Technologies, ICCCT 2021*, pp. 627–633, 2021, doi: 10.1109/ICCCT53315.2021.9711914.
- 940 [26] S. J. Ghoushchi, R. Ranjbarzadeh, A. H. Dadkhah, Y. Pourasad, and M. Bendeche, "An Extended
941 Approach to Predict Retinopathy in Diabetic Patients Using the Genetic Algorithm and Fuzzy C-
942 Means," *Biomed Res Int*, vol. 2021, pp. 1–13, Jun. 2021, doi: 10.1155/2021/5597222.
- 943 [27] A. Naseer, T. Yasir, A. Azhar, T. Shakeel, and K. Zafar, "Computer-Aided Brain Tumor Diagnosis:
944 Performance Evaluation of Deep Learner CNN Using Augmented Brain MRI," *Int J Biomed
945 Imaging*, vol. 2021, 2021, doi: 10.1155/2021/5513500.
- 946 [28] S. Razzaq, M. A. Asghar, and M. J. Khan, "An Improved AI Inspired Brain Tumor Detection," *3rd
947 International Conference on Communication Technologies, ComTech 2021*, pp. 1–6, 2021, doi:
948 10.1109/COMTECH52583.2021.9616648.
- 949 [29] H. E. M. Abdalla and M. Y. Esmail, "Brain Tumor Detection by using Artificial Neural Network,"
950 *2018 International Conference on Computer, Control, Electrical, and Electronics Engineering,
951 ICCCEEE 2018*, Oct. 2018, doi: 10.1109/ICCCEEE.2018.8515763.

- 952 [30] S. Bauer, R. Wiest, L. P. Nolte, and M. Reyes, "A survey of MRI-based medical image analysis for
953 brain tumor studies," *Phys Med Biol*, vol. 58, no. 13, p. R97, Jun. 2013, doi: 10.1088/0031-
954 9155/58/13/R97.
- 955 [31] F. Fraioli and S. Punwani, "Clinical and research applications of simultaneous positron emission
956 tomography and MRI," *British Journal of Radiology*, vol. 87, no. 1033. British Institute of
957 Radiology, Jan. 2014. doi: 10.1259/bjr.20130464.
- 958 [32] A. Tiwari, S. Srivastava, and M. Pant, "Brain tumor segmentation and classification from magnetic
959 resonance images: Review of selected methods from 2014 to 2019," *Pattern Recognit Lett*, vol. 131,
960 pp. 244–260, Mar. 2020, doi: 10.1016/J.PATREC.2019.11.020.
- 961 [33] A. Wadhwa, A. Bhardwaj, and V. Singh Verma, "A review on brain tumor segmentation of MRI
962 images," *Magn Reson Imaging*, vol. 61, pp. 247–259, Sep. 2019, doi: 10.1016/J.MRI.2019.05.043.
- 963 [34] S.-G. Choi, C.-B. Sohn, and P. D. Candidate, "Detection of HGG and LGG Brain Tumors using U-
964 Net," *Medico Legal Update*, vol. 19, no. 1, pp. 560–565, Feb. 2019, doi: 10.37506/MLU.V19I1.978.
- 965 [35] S. Lapointe, A. Perry, and N. A. Butowski, "Primary brain tumours in adults," *The Lancet*, vol. 392,
966 no. 10145, pp. 432–446, Aug. 2018, doi: 10.1016/S0140-6736(18)30990-5.
- 967 [36] C. J. Valvona, H. L. Fillmore, P. B. Nunn, and G. J. Pilkington, "The Regulation and Function of
968 Lactate Dehydrogenase A: Therapeutic Potential in Brain Tumor," *Brain Pathology*, vol. 26, no. 1,
969 pp. 3–17, Jan. 2016, doi: 10.1111/BPA.12299.
- 970 [37] S.-G. Choi, C.-B. Sohn, and P. D. Candidate, "Detection of HGG and LGG Brain Tumors using U-
971 Net," *Medico Legal Update*, vol. 19, no. 1, pp. 560–565, Feb. 2019, doi: 10.37506/MLU.V19I1.978.
- 972 [38] C. I. Hill, C. S. Nixon, J. L. Ruehmeier, and L. M. Wolf, "Brain Tumors," *Phys Ther*, vol. 82, no.
973 5, pp. 496–502, May 2002, doi: 10.1093/PTJ/82.5.496.
- 974 [39] S. Saman and S. Jamjala Narayanan, "Survey on brain tumor segmentation and feature extraction of
975 MR images," *International Journal of Multimedia Information Retrieval 2018 8:2*, vol. 8, no. 2, pp.
976 79–99, Dec. 2018, doi: 10.1007/S13735-018-0162-2.
- 977 [40] S. Bacchi *et al.*, "Deep learning in the detection of high-grade glioma recurrence using multiple MRI
978 sequences: A pilot study," *Journal of Clinical Neuroscience*, vol. 70, pp. 11–13, Dec. 2019, doi:
979 10.1016/J.JOCN.2019.10.003.
- 980 [41] D. A. Hormuth *et al.*, "Translating preclinical MRI methods to clinical oncology," *Journal of*
981 *Magnetic Resonance Imaging*, vol. 50, no. 5, pp. 1377–1392, Nov. 2019, doi: 10.1002/JMRI.26731.
- 982 [42] J. Amin, M. Sharif, N. Gul, M. Yasmin, and S. A. Shad, "Brain tumor classification based on DWT
983 fusion of MRI sequences using convolutional neural network," *Pattern Recognit Lett*, vol. 129, pp.
984 115–122, Jan. 2020, doi: 10.1016/J.PATREC.2019.11.016.
- 985 [43] S. Saman and S. Jamjala Narayanan, "Survey on brain tumor segmentation and feature extraction of
986 MR images," *International Journal of Multimedia Information Retrieval 2018 8:2*, vol. 8, no. 2, pp.
987 79–99, Dec. 2018, doi: 10.1007/S13735-018-0162-2.
- 988 [44] R. Schettini, "A segmentation algorithm for color images," *Pattern Recognit Lett*, vol. 14, no. 6, pp.
989 499–506, Jun. 1993, doi: 10.1016/0167-8655(93)90030-H.

- 990 [45] T. Kumar, J. Park, M. S. Ali, A. F. M. Shahab Uddin, J. H. Ko, and S.-H. Bae, "Binary-Classifiers-
991 Enabled Filters for Semi-Supervised Learning," *IEEE Access*, pp. 1–1, 2021, doi:
992 10.1109/ACCESS.2021.3124200.
- 993 [46] M. Turab, T. Kumar, M. Bendeche, and T. Saber, "Investigating Multi-Feature Selection and
994 Ensembling for Audio Classification," Jun. 2022, doi: 10.48550/arxiv.2206.07511.
- 995 [47] S. Bauer, R. Wiest, L. P. Nolte, and M. Reyes, "A survey of MRI-based medical image analysis for
996 brain tumor studies," *Phys Med Biol*, vol. 58, no. 13, p. R97, Jun. 2013, doi: 10.1088/0031-
997 9155/58/13/R97.
- 998 [48] A. Baghban, M. Kahani, M. A. Nazari, M. H. Ahmadi, and W. M. Yan, "Sensitivity analysis and
999 application of machine learning methods to predict the heat transfer performance of CNT/water
1000 nanofluid flows through coils," *Int J Heat Mass Transf*, vol. 128, pp. 825–835, Jan. 2019, doi:
1001 10.1016/J.IJHEATMASSTRANSFER.2018.09.041.
- 1002 [49] Z. Liu and A. Baghban, "Application of LSSVM for biodiesel production using supercritical ethanol
1003 solvent," <http://dx.doi.org/10.1080/15567036.2017.1380732>, vol. 39, no. 17, pp. 1869–1874, Oct.
1004 2017, doi: 10.1080/15567036.2017.1380732.
- 1005 [50] S. Baseri Saadi, N. Tataei Sarshar, S. Sadeghi, R. Ranjbarzadeh, M. Kooshki Forooshani, and M.
1006 Bendeche, "Investigation of Effectiveness of Shuffled Frog-Leaping Optimizer in Training a
1007 Convolution Neural Network," *J Healthc Eng*, vol. 2022, pp. 1–11, Mar. 2022, doi:
1008 10.1155/2022/4703682.
- 1009 [51] R. Ranjbarzadeh *et al.*, "MRFE-CNN: multi-route feature extraction model for breast tumor
1010 segmentation in Mammograms using a convolutional neural network," *Annals of Operations
1011 Research 2022*, pp. 1–22, May 2022, doi: 10.1007/S10479-022-04755-8.
- 1012 [52] J. Dougherty, R. Kohavi, and M. Sahami, "Supervised and Unsupervised Discretization of
1013 Continuous Features," *Machine Learning Proceedings 1995*, pp. 194–202, Jan. 1995, doi:
1014 10.1016/B978-1-55860-377-6.50032-3.
- 1015 [53] A. Qi *et al.*, "Directional mutation and crossover boosted ant colony optimization with application
1016 to COVID-19 X-ray image segmentation," *Comput Biol Med*, vol. 148, p. 105810, Sep. 2022, doi:
1017 10.1016/J.COMPBIOMED.2022.105810.
- 1018 [54] N. H. Rajini and R. Bhavani, "Classification of MRI brain images using k-nearest neighbor and
1019 artificial neural network," *International Conference on Recent Trends in Information Technology,
1020 ICRTIT 2011*, pp. 563–568, 2011, doi: 10.1109/ICRTIT.2011.5972341.
- 1021 [55] S. Sun and R. Huang, "An adaptive k-nearest neighbor algorithm," *Proceedings - 2010 7th
1022 International Conference on Fuzzy Systems and Knowledge Discovery, FSKD 2010*, vol. 1, pp. 91–
1023 94, 2010, doi: 10.1109/FSKD.2010.5569740.
- 1024 [56] M. Havaei, H. Larochelle, P. Poulin, and P. M. Jodoin, "Within-brain classification for brain tumor
1025 segmentation," *International Journal of Computer Assisted Radiology and Surgery 2015 11:5*, vol.
1026 11, no. 5, pp. 777–788, Nov. 2015, doi: 10.1007/S11548-015-1311-1.
- 1027 [57] G. Cinarer and B. G. Emiroglu, "Classificatin of Brain Tumors by Machine Learning Algorithms,"
1028 *3rd International Symposium on Multidisciplinary Studies and Innovative Technologies, ISMSIT
1029 2019 - Proceedings*, Oct. 2019, doi: 10.1109/ISMSIT.2019.8932878.

- 1030 [58] D. M. Kumar, D. Satyanarayana, and M. N. G. Prasad, "MRI brain tumor detection using optimal
1031 possibilistic fuzzy C-means clustering algorithm and adaptive k-nearest neighbor classifier,"
1032 *Journal of Ambient Intelligence and Humanized Computing* 2020 12:2, vol. 12, no. 2, pp. 2867–
1033 2880, Sep. 2020, doi: 10.1007/S12652-020-02444-7.
- 1034 [59] A. S. Remya Ajai and S. Gopalan, "Analysis of active contours without edge-based segmentation
1035 technique for brain tumor classification using svm and knn classifiers," *Lecture Notes in Electrical
1036 Engineering*, vol. 656, pp. 1–10, 2020, doi: 10.1007/978-981-15-3992-3_1/COVER/.
- 1037 [60] R. H. Ramdlon, E. Martiana Kusumaningtyas, and T. Karlita, "Brain Tumor Classification Using
1038 MRI Images with K-Nearest Neighbor Method," *IES 2019 - International Electronics Symposium:
1039 The Role of Techno-Intelligence in Creating an Open Energy System Towards Energy Democracy,
1040 Proceedings*, pp. 660–667, Sep. 2019, doi: 10.1109/ELECSYM.2019.8901560.
- 1041 [61] V. V. P. Wibowo, Z. Rustam, and J. Pandelaki, "Classification of Brain Tumor Using K-Nearest
1042 Neighbor-Genetic Algorithm and Support Vector Machine-Genetic Algorithm Methods," *2021
1043 International Conference on Decision Aid Sciences and Application, DASA 2021*, pp. 1077–1081,
1044 2021, doi: 10.1109/DASA53625.2021.9682341.
- 1045 [62] A. Shmilovici, "Support Vector Machines," *Data Mining and Knowledge Discovery Handbook*, pp.
1046 231–247, 2009, doi: 10.1007/978-0-387-09823-4_12.
- 1047 [63] H. B. Nandpuru, S. S. Salankar, and V. R. Bora, "MRI brain cancer classification using support
1048 vector machine," *2014 IEEE Students' Conference on Electrical, Electronics and Computer
1049 Science, SCEECS 2014*, 2014, doi: 10.1109/SCEECS.2014.6804439.
- 1050 [64] J. Amin, M. Sharif, M. Yasmin, and S. L. Fernandes, "A distinctive approach in brain tumor
1051 detection and classification using MRI," *Pattern Recognit Lett*, vol. 139, pp. 118–127, Nov. 2020,
1052 doi: 10.1016/J.PATREC.2017.10.036.
- 1053 [65] M. Padlia and J. Sharma, "Fractional sobel filter based brain tumor detection and segmentation using
1054 statistical features and SVM," *Lecture Notes in Electrical Engineering*, vol. 511, pp. 161–175, 2019,
1055 doi: 10.1007/978-981-13-0776-8_15/COVER/.
- 1056 [66] M. O. Khairandish, M. Sharma, V. Jain, J. M. Chatterjee, and N. Z. Jhanjhi, "A Hybrid CNN-SVM
1057 Threshold Segmentation Approach for Tumor Detection and Classification of MRI Brain Images,"
1058 *IRBM*, Jun. 2021, doi: 10.1016/J.IRBM.2021.06.003.
- 1059 [67] C. S. Rao and K. Karunakara, "Efficient Detection and Classification of Brain Tumor using Kernel
1060 based SVM for MRI," *Multimedia Tools and Applications* 2022 81:5, vol. 81, no. 5, pp. 7393–7417,
1061 Jan. 2022, doi: 10.1007/S11042-021-11821-Z.
- 1062 [68] M. H. O. Rashid, M. A. Mamun, M. A. Hossain, and M. P. Uddin, "Brain Tumor Detection Using
1063 Anisotropic Filtering, SVM Classifier and Morphological Operation from MR Images,"
1064 *International Conference on Computer, Communication, Chemical, Material and Electronic
1065 Engineering, IC4ME2 2018*, Sep. 2018, doi: 10.1109/IC4ME2.2018.8465613.
- 1066 [69] S. Deepak and P. M. Ameer, "Automated Categorization of Brain Tumor from MRI Using CNN
1067 features and SVM," *Journal of Ambient Intelligence and Humanized Computing* 2020 12:8, vol. 12,
1068 no. 8, pp. 8357–8369, Oct. 2020, doi: 10.1007/S12652-020-02568-W.

- 1069 [70] Y. Qi, "Random Forest for Bioinformatics," *Ensemble Machine Learning*, pp. 307–323, 2012, doi:
1070 10.1007/978-1-4419-9326-7_11.
- 1071 [71] T. M. Oshiro, P. S. Perez, and J. A. Baranauskas, "How many trees in a random forest?," *Lecture*
1072 *Notes in Computer Science (including subseries Lecture Notes in Artificial Intelligence and Lecture*
1073 *Notes in Bioinformatics)*, vol. 7376 LNAI, pp. 154–168, 2012, doi: 10.1007/978-3-642-31537-
1074 4_13/COVER.
- 1075 [72] L. Lefkovits, S. Lefkovits, and L. Szilágyi, "Brain Tumor Segmentation with Optimized Random
1076 Forest," *Lecture Notes in Computer Science (including subseries Lecture Notes in Artificial*
1077 *Intelligence and Lecture Notes in Bioinformatics)*, vol. 10154 LNCS, pp. 88–99, Oct. 2016, doi:
1078 10.1007/978-3-319-55524-9_9.
- 1079 [73] A. Ellwaa *et al.*, "Brain tumor segmantation using random forest trained on iteratively selected
1080 patients," *Lecture Notes in Computer Science (including subseries Lecture Notes in Artificial*
1081 *Intelligence and Lecture Notes in Bioinformatics)*, vol. 10154 LNCS, pp. 129–137, 2016, doi:
1082 10.1007/978-3-319-55524-9_13/COVER/.
- 1083 [74] R. Anitha and D. Siva Sundhara Raja, "Development of computer-aided approach for brain tumor
1084 detection using random forest classifier," *Int J Imaging Syst Technol*, vol. 28, no. 1, pp. 48–53, Mar.
1085 2018, doi: 10.1002/IMA.22255.
- 1086 [75] T. Yang, J. Song, and L. Li, "A deep learning model integrating SK-TPCNN and random forests for
1087 brain tumor segmentation in MRI," *Biocybern Biomed Eng*, vol. 39, no. 3, pp. 613–623, Jul. 2019,
1088 doi: 10.1016/J.BBE.2019.06.003.
- 1089 [76] R. Rajagopal, "Glioma brain tumor detection and segmentation using weighting random forest
1090 classifier with optimized ant colony features," *Int J Imaging Syst Technol*, vol. 29, no. 3, pp. 353–
1091 359, Sep. 2019, doi: 10.1002/IMA.22331.
- 1092 [77] A. J. Myles, R. N. Feudale, Y. Liu, N. A. Woody, and S. D. Brown, "An introduction to decision
1093 tree modeling," *J Chemom*, vol. 18, no. 6, pp. 275–285, Jun. 2004, doi: 10.1002/CEM.873.
- 1094 [78] W. Wang, A. Tu, and F. Bergholm, "Improved Minimum Spanning Tree based Image Segmentation
1095 with Guided Matting," *KSII Transactions on Internet and Information Systems (TIIS)*, vol. 16, no.
1096 1, pp. 211–230, Jan. 2022, doi: 10.3837/TIIS.2022.01.012.
- 1097 [79] Y. Y. Song and Y. Lu, "Decision tree methods: applications for classification and prediction,"
1098 *Shanghai Arch Psychiatry*, vol. 27, no. 2, p. 130, Apr. 2015, doi: 10.11919/J.ISSN.1002-
1099 0829.215044.
- 1100 [80] "Tumor Detection and Classification using Decision Tree in Brain MRI | Semantic Scholar."
- 1101 [81] A. Chaddad, P. O. Zinn, and R. R. Colen, "Brain tumor identification using Gaussian Mixture Model
1102 features and Decision Trees classifier," *2014 48th Annual Conference on Information Sciences and*
1103 *Systems, CISS 2014*, 2014, doi: 10.1109/CISS.2014.6814077.
- 1104 [82] L. Hussain, S. Saeed, I. A. Awan, A. Idris, M. S. A. Nadeem, and Q.-A. Chaudhry, "Detecting Brain
1105 Tumor using Machines Learning Techniques Based on Different Features Extracting Strategies,"
1106 *Current Medical Imaging Formerly Current Medical Imaging Reviews*, vol. 15, no. 6, pp. 595–606,
1107 Jul. 2019, doi: 10.2174/1573405614666180718123533.

- 1108 [83] M. Thayumanavan and A. Ramasamy, "An efficient approach for brain tumor detection and
1109 segmentation in MR brain images using random forest classifier.,"
1110 <https://doi.org/10.1177/1063293X211010542>, vol. 29, no. 3, pp. 266–274, Apr. 2021, doi:
1111 10.1177/1063293X211010542.
- 1112 [84] P. Rajendran and M. Madheswaran, "Hybrid Medical Image Classification Using Association Rule
1113 Mining with Decision Tree Algorithm," vol. 2, Jan. 2010, doi: 10.48550/arxiv.1001.3503.
- 1114 [85] Z. Zhang, "Artificial Neural Network," *Multivariate Time Series Analysis in Climate and
1115 Environmental Research*, pp. 1–35, 2018, doi: 10.1007/978-3-319-67340-0_1.
- 1116 [86] S. Tang and F. Yu, "Construction and verification of retinal vessel segmentation algorithm for color
1117 fundus image under BP neural network model," *Journal of Supercomputing*, vol. 77, no. 4, pp.
1118 3870–3884, Apr. 2021, doi: 10.1007/S11227-020-03422-8/FIGURES/4.
- 1119 [87] B. He *et al.*, "Image segmentation algorithm of lung cancer based on neural network model," *Expert
1120 Syst*, vol. 39, no. 3, p. e12822, Mar. 2022, doi: 10.1111/EXSY.12822.
- 1121 [88] M. Mishra and M. Srivastava, "A view of Artificial Neural Network," *2014 International
1122 Conference on Advances in Engineering and Technology Research, ICAETR 2014*, 2014, doi:
1123 10.1109/ICAETR.2014.7012785.
- 1124 [89] T. Chithambaram and K. Perumal, "Brain tumor segmentation using genetic algorithm and ANN
1125 techniques," *IEEE International Conference on Power, Control, Signals and Instrumentation
1126 Engineering, ICPCSI 2017*, pp. 970–982, Jun. 2018, doi: 10.1109/ICPCSI.2017.8391855.
- 1127 [90] Virupakshappa and B. Amarapur, "Computer-aided diagnosis applied to MRI images of brain tumor
1128 using cognition based modified level set and optimized ANN classifier," *Multimedia Tools and
1129 Applications 2018 79:5*, vol. 79, no. 5, pp. 3571–3599, Jun. 2018, doi: 10.1007/S11042-018-6176-
1130 1.
- 1131 [91] Virupakshappa and B. Amarapur, "An Automated Approach for Brain Tumor Identification using
1132 ANN Classifier," *International Conference on Current Trends in Computer, Electrical, Electronics
1133 and Communication, CTCEEC 2017*, pp. 1011–1016, Sep. 2018, doi:
1134 10.1109/CTCEEC.2017.8455154.
- 1135 [92] G. I. Webb, "Naïve Bayes," *Encyclopedia of Machine Learning and Data Mining*, pp. 1–2, 2016,
1136 doi: 10.1007/978-1-4899-7502-7_581-1.
- 1137 [93] W. Li, G. G. Wang, and A. H. Gandomi, "A Survey of Learning-Based Intelligent Optimization
1138 Algorithms," *Archives of Computational Methods in Engineering 2021 28:5*, vol. 28, no. 5, pp.
1139 3781–3799, Feb. 2021, doi: 10.1007/S11831-021-09562-1.
- 1140 [94] L. Jiang, H. Zhang, and Z. Cai, "A novel bayes model: Hidden naive bayes," *IEEE Trans Knowl
1141 Data Eng*, vol. 21, no. 10, pp. 1361–1371, Oct. 2009, doi: 10.1109/TKDE.2008.234.
- 1142 [95] G. Kaur and A. Oberoi, "Novel Approach for Brain Tumor Detection Based on Naïve Bayes
1143 Classification," *Advances in Intelligent Systems and Computing*, vol. 1042, pp. 451–462, 2020, doi:
1144 10.1007/978-981-32-9949-8_31/COVER/.

- 1145 [96] A. R. Raju, P. Suresh, and R. R. Rao, "Bayesian HCS-based multi-SVNN: A classification approach
1146 for brain tumor segmentation and classification using Bayesian fuzzy clustering," *Biocybern Biomed*
1147 *Eng*, vol. 38, no. 3, pp. 646–660, Jan. 2018, doi: 10.1016/J.BBE.2018.05.001.
- 1148 [97] E. E. Ulku and A. Y. Camurcu, "Computer aided brain tumor detection with histogram equalization
1149 and morphological image processing techniques," *2013 International Conference on Electronics,*
1150 *Computer and Computation, ICECCO 2013*, pp. 48–51, 2013, doi:
1151 10.1109/ICECCO.2013.6718225.
- 1152 [98] T. Kohonen, "Learning Vector Quantization," pp. 245–261, 2001, doi: 10.1007/978-3-642-56927-
1153 2_6.
- 1154 [99] D. Nova and P. A. Estévez, "A review of learning vector quantization classifiers," *Neural*
1155 *Computing and Applications 2013 25:3*, vol. 25, no. 3, pp. 511–524, Dec. 2013, doi:
1156 10.1007/S00521-013-1535-3.
- 1157 [100] T. Liu, C. Chen, X. Shi, and C. Liu, "Evaluation of Raman spectra of human brain tumor tissue
1158 using the learning vector quantization neural network," *Laser Phys*, vol. 26, no. 5, p. 055606, Apr.
1159 2016, doi: 10.1088/1054-660X/26/5/055606.
- 1160 [101] R. Sonavane, P. Sonar, and S. Sutar, "Classification of MRI brain tumor and mammogram images
1161 using learning vector quantization neural network," *Proceedings of 2017 3rd IEEE International*
1162 *Conference on Sensing, Signal Processing and Security, ICSSS 2017*, pp. 301–307, Oct. 2017, doi:
1163 10.1109/SSPS.2017.8071610.
- 1164 [102] R. S. Sonavane and A. S. Sonavane, "Classification of MRI brain tumor and mammogram images
1165 using adaboost and learning vector quantization neural network," *2020 International Conference on*
1166 *Convergence to Digital World - Quo Vadis, ICCDW 2020*, Feb. 2020, doi:
1167 10.1109/ICCDW45521.2020.9318645.
- 1168 [103] T. Hastie, R. Tibshirani, and J. Friedman, "Unsupervised Learning," Springer, New York, NY, 2009,
1169 pp. 485–585. doi: 10.1007/978-0-387-84858-7_14.
- 1170 [104] H. Su *et al.*, "Multilevel threshold image segmentation for COVID-19 chest radiography: A
1171 framework using horizontal and vertical multiverse optimization," *Comput Biol Med*, vol. 146, p.
1172 105618, Jul. 2022, doi: 10.1016/J.COMPBIOMED.2022.105618.
- 1173 [105] S. Anari, N. Tataei Sarshar, N. Mahjoori, S. Dorosti, and A. Rezaie, "Review of Deep Learning
1174 Approaches for Thyroid Cancer Diagnosis," *Math Probl Eng*, vol. 2022, pp. 1–8, Aug. 2022, doi:
1175 10.1155/2022/5052435.
- 1176 [106] D. Gao, G. G. Wang, and W. Pedrycz, "Solving Fuzzy Job-Shop Scheduling Problem Using de
1177 Algorithm Improved by a Selection Mechanism," *IEEE Transactions on Fuzzy Systems*, vol. 28, no.
1178 12, pp. 3265–3275, Dec. 2020, doi: 10.1109/TFUZZ.2020.3003506.
- 1179 [107] G. G. Wang, D. Gao, and W. Pedrycz, "Solving Multi-Objective Fuzzy Job-shop Scheduling
1180 Problem by a Hybrid Adaptive Differential Evolution Algorithm," *IEEE Trans Industr Inform*, Dec.
1181 2022, doi: 10.1109/TII.2022.3165636.
- 1182 [108] M. A. T. Figueiredo and A. K. Jain, "Unsupervised learning of finite mixture models," *IEEE Trans*
1183 *Pattern Anal Mach Intell*, vol. 24, no. 3, pp. 381–396, Mar. 2002, doi: 10.1109/34.990138.

- 1184 [109] K. Krishna and M. N. Murty, "Genetic K-means algorithm," *IEEE Transactions on Systems, Man,*
1185 *and Cybernetics, Part B: Cybernetics*, vol. 29, no. 3, pp. 433–439, 1999, doi: 10.1109/3477.764879.
- 1186 [110] A. Likas, N. Vlassis, and J. J. Verbeek, "The global k-means clustering algorithm," *Pattern*
1187 *Recognit*, vol. 36, no. 2, pp. 451–461, Feb. 2003, doi: 10.1016/S0031-3203(02)00060-2.
- 1188 [111] R. Khilkhal and M. Ismael, "Brain Tumor Segmentation Utilizing Thresholding and K-Means
1189 Clustering," pp. 43–48, Jun. 2022, doi: 10.1109/MICEST54286.2022.9790103.
- 1190 [112] M. K. Islam, M. S. Ali, M. S. Miah, M. M. Rahman, M. S. Alam, and M. A. Hossain, "Brain tumor
1191 detection in MR image using superpixels, principal component analysis and template based K-
1192 means clustering algorithm," *Machine Learning with Applications*, vol. 5, p. 100044, Sep. 2021,
1193 doi: 10.1016/J.MLWA.2021.100044.
- 1194 [113] D. M. Kumar, D. Satyanarayana, and M. N. G. Prasad, "An improved Gabor wavelet transform and
1195 rough K-means clustering algorithm for MRI brain tumor image segmentation," *Multimedia Tools*
1196 *and Applications 2020 80:5*, vol. 80, no. 5, pp. 6939–6957, Oct. 2020, doi: 10.1007/S11042-020-
1197 09635-6.
- 1198 [114] T. C. Havens, J. C. Bezdek, C. Leckie, L. O. Hall, and M. Palaniswami, "Fuzzy c-Means algorithms
1199 for very large data," *IEEE Transactions on Fuzzy Systems*, vol. 20, no. 6, pp. 1130–1146, 2012, doi:
1200 10.1109/TFUZZ.2012.2201485.
- 1201 [115] S. Askari, "Fuzzy C-Means clustering algorithm for data with unequal cluster sizes and
1202 contaminated with noise and outliers: Review and development," *Expert Syst Appl*, vol. 165, p.
1203 113856, Mar. 2021, doi: 10.1016/J.ESWA.2020.113856.
- 1204 [116] H. Izakian and A. Abraham, "Fuzzy C-means and fuzzy swarm for fuzzy clustering problem,"
1205 *Expert Syst Appl*, vol. 38, no. 3, pp. 1835–1838, Mar. 2011, doi: 10.1016/J.ESWA.2010.07.112.
- 1206 [117] R. Sindhiya Devi, B. Perumal, and M. Pallikonda Rajasekaran, "A hybrid deep learning based brain
1207 tumor classification and segmentation by stationary wavelet packet transform and adaptive kernel
1208 fuzzy c means clustering," *Advances in Engineering Software*, vol. 170, p. 103146, Aug. 2022, doi:
1209 10.1016/J.ADVENGSOFT.2022.103146.
- 1210 [118] S. Debnath, F. A. Talukdar, and M. Islam, "Combination of contrast enhanced fuzzy c-means
1211 (CEFCM) clustering and pixel based voxel mapping technique (PBVMT) for three dimensional
1212 brain tumour detection," *Journal of Ambient Intelligence and Humanized Computing 2020 12:2*,
1213 vol. 12, no. 2, pp. 2421–2433, Aug. 2020, doi: 10.1007/S12652-020-02366-4.
- 1214 [119] C. J. J. Sheela and G. Suganthi, "Accurate MRI brain tumor segmentation based on rotating
1215 triangular section with fuzzy C- means optimization," *Sādhanā 2021 46:4*, vol. 46, no. 4, pp. 1–20,
1216 Oct. 2021, doi: 10.1007/S12046-021-01744-8.
- 1217 [120] M. Soleymanifard and M. Hamghalam, "Multi-stage glioma segmentation for tumour grade
1218 classification based on multiscale fuzzy C-means," *Multimedia Tools and Applications 2022 81:6*,
1219 vol. 81, no. 6, pp. 8451–8470, Feb. 2022, doi: 10.1007/S11042-022-12326-Z.
- 1220 [121] X. T. Yuan, B. G. Hu, and R. He, "Agglomerative mean-shift clustering," *IEEE Trans Knowl Data*
1221 *Eng*, vol. 24, no. 2, pp. 209–219, 2012, doi: 10.1109/TKDE.2010.232.

- 1222 [122] R. Ranjbarzadeh and S. B. Saadi, "Automated liver and tumor segmentation based on concave and
1223 convex points using fuzzy c-means and mean shift clustering," *Measurement*, vol. 150, p. 107086,
1224 Jan. 2020, doi: 10.1016/J.MEASUREMENT.2019.107086.
- 1225 [123] K. L. Wu and M. S. Yang, "Mean shift-based clustering," *Pattern Recognit*, vol. 40, no. 11, pp.
1226 3035–3052, Nov. 2007, doi: 10.1016/J.PATCOG.2007.02.006.
- 1227 [124] R. B. Vallabhaneni and V. Rajesh, "Brain tumour detection using mean shift clustering and GLCM
1228 features with edge adaptive total variation denoising technique," *Alexandria Engineering Journal*,
1229 vol. 57, no. 4, pp. 2387–2392, Dec. 2018, doi: 10.1016/J.AEJ.2017.09.011.
- 1230 [125] B. Singh and P. Aggarwal, "Detection of brain tumor using modified mean-shift based fuzzy c-mean
1231 segmentation from MRI Images," *2017 8th IEEE Annual Information Technology, Electronics and
1232 Mobile Communication Conference, IEMCON 2017*, pp. 536–545, Nov. 2017, doi:
1233 10.1109/IEMCON.2017.8117123.
- 1234 [126] J. H. Kim, S. Lee, G. S. Lee, Y. S. Park, and Y. P. Hong, "Using a Method Based on a Modified K-
1235 Means Clustering and Mean Shift Segmentation to Reduce File Sizes and Detect Brain Tumors from
1236 Magnetic Resonance (MRI) Images," *Wireless Personal Communications 2016 89:3*, vol. 89, no. 3,
1237 pp. 993–1008, Jun. 2016, doi: 10.1007/S11277-016-3420-8.
- 1238 [127] F. Murtagh and P. Contreras, "Algorithms for hierarchical clustering: an overview," *Wiley
1239 Interdiscip Rev Data Min Knowl Discov*, vol. 2, no. 1, pp. 86–97, Jan. 2012, doi: 10.1002/WIDM.53.
- 1240 [128] F. Nielsen, "Hierarchical Clustering," pp. 195–211, 2016, doi: 10.1007/978-3-319-21903-5_8.
- 1241 [129] T. Hiratsuka *et al.*, "Hierarchical Cluster and Region of Interest Analyses Based on Mass
1242 Spectrometry Imaging of Human Brain Tumours," *Scientific Reports 2020 10:1*, vol. 10, no. 1, pp.
1243 1–11, Apr. 2020, doi: 10.1038/s41598-020-62176-8.
- 1244 [130] G. Tamilmani and S. Sivakumari, "Early detection of brain cancer using association allotment
1245 hierarchical clustering," *Int J Imaging Syst Technol*, vol. 29, no. 4, pp. 617–632, Dec. 2019, doi:
1246 10.1002/IMA.22346.
- 1247 [131] K. Khan, S. U. Rehman, K. Aziz, S. Fong, S. Sarasvady, and A. Vishwa, "DBSCAN: Past, present
1248 and future," *5th International Conference on the Applications of Digital Information and Web
1249 Technologies, ICADIWT 2014*, pp. 232–238, 2014, doi: 10.1109/ICADIWT.2014.6814687.
- 1250 [132] E. Schubert, J. Sander, M. Ester, H. P. Kriegel, and X. Xu, "DBSCAN Revisited, Revisited," *ACM
1251 Transactions on Database Systems (TODS)*, vol. 42, no. 3, Jul. 2017, doi: 10.1145/3068335.
- 1252 [133] "ANALYSIS OF BRAIN TUMOR CLASSIFICATION BY USING MULTIPLE CLUSTERING
1253 ALGORITHMS | Semantic Scholar."
- 1254 [134] "[PDF] Segmentation of Brain Tumour from MRI image – Analysis of K-means and DBSCAN
1255 Clustering | Semantic Scholar."
- 1256 [135] M. A. T. Figueiredo and A. K. Jain, "Unsupervised learning of finite mixture models," *IEEE Trans
1257 Pattern Anal Mach Intell*, vol. 24, no. 3, pp. 381–396, Mar. 2002, doi: 10.1109/34.990138.
- 1258 [136] A. Chaddad, "Automated feature extraction in brain tumor by magnetic resonance imaging using
1259 Gaussian mixture models," *Journal of Biomedical Imaging*, vol. 2015, Jan. 2015, doi:
1260 10.1155/2015/868031.

- 1261 [137] A. A. Pravitasari *et al.*, “MRI-based brain tumor segmentation using Gaussian mixture model with
1262 reversible jump Markov chain Monte Carlo algorithm,” *AIP Conf Proc*, vol. 2194, no. 1, p. 020085,
1263 Dec. 2019, doi: 10.1063/1.5139817.
- 1264 [138] S. Bonte, I. Goethals, and R. Van Holen, “Machine learning based brain tumour segmentation on
1265 limited data using local texture and abnormality,” *Comput Biol Med*, vol. 98, pp. 39–47, Jul. 2018,
1266 doi: 10.1016/J.COMPBIOMED.2018.05.005.
- 1267 [139] N. B. Bahadure, A. K. Ray, and H. P. Thethi, “Comparative Approach of MRI-Based Brain Tumor
1268 Segmentation and Classification Using Genetic Algorithm,” *Journal of Digital Imaging 2018 31:4*,
1269 vol. 31, no. 4, pp. 477–489, Jan. 2018, doi: 10.1007/S10278-018-0050-6.
- 1270 [140] A. Srinivasa Reddy and P. Chenna Reddy, “MRI brain tumor segmentation and prediction using
1271 modified region growing and adaptive SVM,” *Soft Computing 2021 25:5*, vol. 25, no. 5, pp. 4135–
1272 4148, Jan. 2021, doi: 10.1007/S00500-020-05493-4.
- 1273 [141] X. Xie, “A K-Nearest Neighbor Technique for Brain Tumor Segmentation Using Minkowski
1274 Distance,” *J Med Imaging Health Inform*, vol. 8, no. 2, pp. 180–185, Jan. 2018, doi:
1275 10.1166/JMIHI.2018.2285.
- 1276 [142] P. M. Siva Raja and A. V. rani, “Brain tumor classification using a hybrid deep autoencoder with
1277 Bayesian fuzzy clustering-based segmentation approach,” *Biocybern Biomed Eng*, vol. 40, no. 1,
1278 pp. 440–453, Jan. 2020, doi: 10.1016/J.BBE.2020.01.006.
- 1279 [143] U. Ilhan and A. Ilhan, “Brain tumor segmentation based on a new threshold approach,” *Procedia
1280 Comput Sci*, vol. 120, pp. 580–587, Jan. 2017, doi: 10.1016/J.PROCS.2017.11.282.
- 1281 [144] A. Aslam, E. Khan, and M. M. S. Beg, “Improved Edge Detection Algorithm for Brain Tumor
1282 Segmentation,” *Procedia Comput Sci*, vol. 58, pp. 430–437, Jan. 2015, doi:
1283 10.1016/J.PROCS.2015.08.057.
- 1284 [145] A. Kermi, K. Andjouh, and F. Zidane, “Fully automated brain tumour segmentation system in 3D-
1285 MRI using symmetry analysis of brain and level sets,” *IET Image Process*, vol. 12, no. 11, pp. 1964–
1286 1971, Nov. 2018, doi: 10.1049/IET-IPR.2017.1124.
- 1287 [146] C. J. J. Sheela and G. Suganthi, “Morphological edge detection and brain tumor segmentation in
1288 Magnetic Resonance (MR) images based on region growing and performance evaluation of
1289 modified Fuzzy C-Means (FCM) algorithm,” *Multimedia Tools and Applications 2020 79:25*, vol.
1290 79, no. 25, pp. 17483–17496, Feb. 2020, doi: 10.1007/S11042-020-08636-9.
- 1291 [147] A. R. Khan, S. Khan, M. Harouni, R. Abbasi, S. Iqbal, and Z. Mehmood, “Brain tumor segmentation
1292 using K-means clustering and deep learning with synthetic data augmentation for classification,”
1293 *Microsc Res Tech*, vol. 84, no. 7, pp. 1389–1399, Jul. 2021, doi: 10.1002/JEMT.23694.
- 1294 [148] F. ŞİŞİK and E. SERT, “Brain tumor segmentation approach based on the extreme learning machine
1295 and significantly fast and robust fuzzy C-means clustering algorithms running on Raspberry Pi
1296 hardware,” *Med Hypotheses*, vol. 136, p. 109507, Mar. 2020, doi: 10.1016/J.MEHY.2019.109507.
- 1297 [149] A. Khosravianian, M. Rahmanimanesh, P. Keshavarzi, and S. Mozaffari, “Fast Level set Method for
1298 Glioma Brain Tumor Segmentation based on Superpixel Fuzzy Clustering and Lattice Boltzmann
1299 Method,” *Comput Methods Programs Biomed*, vol. 198, p. 105809, Oct. 2020, doi:
1300 10.1016/j.cmpb.2020.105809.

- 1301 [150] K. Suzuki, "Overview of deep learning in medical imaging," *Radiological Physics and Technology*
1302 *2017 10:3*, vol. 10, no. 3, pp. 257–273, Jul. 2017, doi: 10.1007/S12194-017-0406-5.
- 1303 [151] M. T. S. T. R. B. and M. B. Teerath Kumar *et al.*, "Forged Character Detection Datasets: Passports,
1304 Driving Licences and Visa Stickers," *International Journal of Artificial Intelligence*
1305 *Applications(IJAIA), Vol.13,No.2*, vol. 13, no. 2, p. 21, Mar. 2022, doi: 10.5121/IJAIA.2022.13202.
- 1306 [152] A. Aiman, Y. Shen, M. Bendeche, I. Inayat, and T. Kumar, "AUDD: Audio Urdu Digits Dataset
1307 for Automatic Audio Urdu Digit Recognition," *Applied Sciences 2021, Vol. 11, Page 8842*, vol. 11,
1308 no. 19, p. 8842, Sep. 2021, doi: 10.3390/APP11198842.
- 1309 [153] 박진배*, T. Kumar, 경희대학교배성호, J. Park, and S.-H. Bae, "Search of an Optimal Sound
1310 Augmentation Policy for Environmental Sound Classification with Deep Neural Networks,"
1311 *Proceedings of the Korean Society of Broadcast Engineers Conference*, pp. 18–21, 2020.
- 1312 [154] S. Aleem, T. Kumar, S. Little, M. Bendeche, R. Brennan, and K. McGuinness, "Random Data
1313 Augmentation based Enhancement: A Generalized Enhancement Approach for Medical Datasets."
1314 Dec. 17, 2021.
- 1315 [155] M. I. Razzak, S. Naz, and A. Zaib, "Deep Learning for Medical Image Processing: Overview,
1316 Challenges and the Future BT - Classification in BioApps: Automation of Decision Making,"
1317 *Springer*, vol. 26, pp. 323–350, 2018.
- 1318 [156] R. Ranjbarzadeh *et al.*, "Nerve optic segmentation in CT images using a deep learning model and a
1319 texture descriptor," *Complex & Intelligent Systems 2022*, pp. 1–15, Feb. 2022, doi: 10.1007/S40747-
1320 022-00694-W.
- 1321 [157] S. Wang *et al.*, "Multi-Scale Context-Guided Deep Network for Automated Lesion Segmentation
1322 with Endoscopy Images of Gastrointestinal Tract," *IEEE J Biomed Health Inform*, vol. 25, no. 2,
1323 pp. 514–525, Feb. 2021, doi: 10.1109/JBHI.2020.2997760.
- 1324 [158] S. Albawi, T. A. Mohammed, and S. Al-Zawi, "Understanding of a convolutional neural network,"
1325 in *Proceedings of 2017 International Conference on Engineering and Technology, ICET 2017*, Mar.
1326 2018, vol. 2018-Janua, pp. 1–6. doi: 10.1109/ICEngTechnol.2017.8308186.
- 1327 [159] R. Yamashita, M. Nishio, R. K. G. Do, and K. Togashi, "Convolutional neural networks: an
1328 overview and application in radiology," *Insights into Imaging*, vol. 9, no. 4. Springer Verlag, pp.
1329 611–629, Aug. 2018. doi: 10.1007/s13244-018-0639-9.
- 1330 [160] I. A. El Kader, G. Xu, Z. Shuai, S. Saminu, I. Javaid, and I. S. Ahmad, "Differential Deep
1331 Convolutional Neural Network Model for Brain Tumor Classification," *Brain Sciences 2021, Vol.*
1332 *11, Page 352*, vol. 11, no. 3, p. 352, Mar. 2021, doi: 10.3390/BRAINSCI11030352.
- 1333 [161] N. Bacanin, T. Bezdán, K. Venkatachalam, and F. Al-Turjman, "Optimized convolutional neural
1334 network by firefly algorithm for magnetic resonance image classification of glioma brain tumor
1335 grade," *Journal of Real-Time Image Processing 2021 18:4*, vol. 18, no. 4, pp. 1085–1098, Apr.
1336 2021, doi: 10.1007/S11554-021-01106-X.
- 1337 [162] J. Wang *et al.*, "DFP-ResUNet: Convolutional Neural Network with a Dilated Convolutional Feature
1338 Pyramid for Multimodal Brain Tumor Segmentation," *Comput Methods Programs Biomed*, vol.
1339 208, p. 106208, Sep. 2021, doi: 10.1016/J.CMPB.2021.106208.

- 1340 [163] A. Gurunathan and B. Krishnan, "Detection and diagnosis of brain tumors using deep learning
1341 convolutional neural networks," *Int J Imaging Syst Technol*, vol. 31, no. 3, pp. 1174–1184, Sep.
1342 2021, doi: 10.1002/IMA.22532.
- 1343 [164] T. Mikolov, S. Kombrink, L. Burget, J. Černocký, and S. Khudanpur, "Extensions of recurrent
1344 neural network language model," *ICASSP, IEEE International Conference on Acoustics, Speech
1345 and Signal Processing - Proceedings*, pp. 5528–5531, 2011, doi: 10.1109/ICASSP.2011.5947611.
- 1346 [165] M. Lukoševičius and H. Jaeger, "Reservoir computing approaches to recurrent neural network
1347 training," *Comput Sci Rev*, vol. 3, no. 3, pp. 127–149, Aug. 2009, doi:
1348 10.1016/J.COSREV.2009.03.005.
- 1349 [166] A. C. Tsoi, "Recurrent neural network architectures: An overview," pp. 1–26, 1998, doi:
1350 10.1007/BFB0053993.
- 1351 [167] J. G. SivaSai, P. N. Srinivasu, M. N. Sindhuri, K. Rohitha, and S. Deepika, "An automated
1352 segmentation of brain MR image through fuzzy recurrent neural network," *Studies in Computational
1353 Intelligence*, vol. 903, pp. 163–179, 2021, doi: 10.1007/978-981-15-5495-7_9/COVER/.
- 1354 [168] Y. Zhou *et al.*, "Holistic brain tumor screening and classification based on densenet and recurrent
1355 neural network," *Lecture Notes in Computer Science (including subseries Lecture Notes in Artificial
1356 Intelligence and Lecture Notes in Bioinformatics)*, vol. 11383 LNCS, pp. 208–217, 2019, doi:
1357 10.1007/978-3-030-11723-8_21/COVER/.
- 1358 [169] S. S. Begum and D. R. Lakshmi, "Combining optimal wavelet statistical texture and recurrent neural
1359 network for tumour detection and classification over MRI," *Multimedia Tools and Applications
1360 2020 79:19*, vol. 79, no. 19, pp. 14009–14030, Feb. 2020, doi: 10.1007/S11042-020-08643-W.
- 1361 [170] G. Van Houdt, C. Mosquera, and G. Nápoles, "A review on the long short-term memory model,"
1362 *Artificial Intelligence Review 2020 53:8*, vol. 53, no. 8, pp. 5929–5955, May 2020, doi:
1363 10.1007/S10462-020-09838-1.
- 1364 [171] A. Graves, "Long Short-Term Memory," pp. 37–45, 2012, doi: 10.1007/978-3-642-24797-2_4.
- 1365 [172] E. Dandil and S. Karaca, "Detection of pseudo brain tumors via stacked LSTM neural networks
1366 using MR spectroscopy signals," *Biocybern Biomed Eng*, vol. 41, no. 1, pp. 173–195, Jan. 2021,
1367 doi: 10.1016/J.BBE.2020.12.003.
- 1368 [173] F. Xu, H. Ma, J. Sun, R. Wu, X. Liu, and Y. Kong, "LSTM Multi-modal UNet for Brain Tumor
1369 Segmentation," *2019 IEEE 4th International Conference on Image, Vision and Computing, ICIVC
1370 2019*, pp. 236–240, Jul. 2019, doi: 10.1109/ICIVC47709.2019.8981027.
- 1371 [174] I. Shahzadi, F. Meriadeau, T. B. Tang, and A. Quyyum, "CNN-LSTM: Cascaded framework for
1372 brain tumour classification," *2018 IEEE EMBS Conference on Biomedical Engineering and
1373 Sciences, IECBES 2018 - Proceedings*, pp. 633–637, Jan. 2019, doi:
1374 10.1109/IECBES.2018.8626704.
- 1375 [175] A. Creswell, T. White, V. Dumoulin, K. Arulkumaran, B. Sengupta, and A. A. Bharath, "Generative
1376 Adversarial Networks: An Overview," *IEEE Signal Process Mag*, vol. 35, no. 1, pp. 53–65, Jan.
1377 2018, doi: 10.1109/MSP.2017.2765202.

- 1378 [176] K. Wang, C. Gou, Y. Duan, Y. Lin, X. Zheng, and F. Y. Wang, "Generative adversarial networks:
1379 Introduction and outlook," *IEEE/CAA Journal of Automatica Sinica*, vol. 4, no. 4, pp. 588–598, Oct.
1380 2017, doi: 10.1109/JAS.2017.7510583.
- 1381 [177] S. Nema, A. Dudhane, S. Murala, and S. Naidu, "RescueNet: An unpaired GAN for brain tumor
1382 segmentation," *Biomed Signal Process Control*, vol. 55, p. 101641, Jan. 2020, doi:
1383 10.1016/J.BSPC.2019.101641.
- 1384 [178] G. Neelima, D. R. Chigurukota, B. Maram, and B. Girirajan, "Optimal DeepMRSeg based tumor
1385 segmentation with GAN for brain tumor classification," *Biomed Signal Process Control*, vol. 74, p.
1386 103537, Apr. 2022, doi: 10.1016/J.BSPC.2022.103537.
- 1387 [179] M. Rezaei, H. Yang, and C. Meinel, "Voxel-GAN: Adversarial framework for learning imbalanced
1388 brain tumor segmentation," *Lecture Notes in Computer Science (including subseries Lecture Notes*
1389 *in Artificial Intelligence and Lecture Notes in Bioinformatics)*, vol. 11384 LNCS, pp. 321–333,
1390 2019, doi: 10.1007/978-3-030-11726-9_29/COVER/.
- 1391 [180] Y. Hua, J. Guo, and H. Zhao, "Deep Belief Networks and deep learning," *Proceedings of 2015*
1392 *International Conference on Intelligent Computing and Internet of Things, ICIT 2015*, pp. 1–4, May
1393 2015, doi: 10.1109/ICAIOT.2015.7111524.
- 1394 [181] A. Kharrat and M. Néji, "Classification of brain tumors using personalized deep belief networks on
1395 MRImages: PDBN-MRI," <https://doi.org/10.1117/12.2522848>, vol. 11041, pp. 713–721, Mar.
1396 2019, doi: 10.1117/12.2522848.
- 1397 [182] A. Ratna Raju, S. Pabboju, and R. Rajeswara Rao, "Hybrid active contour model and deep belief
1398 network based approach for brain tumor segmentation and classification," *Sensor Review*, vol. 39,
1399 no. 4, pp. 473–487, Jul. 2019, doi: 10.1108/SR-01-2018-0008/FULL/XML.
- 1400 [183] M. Tschannen, O. Bachem, and M. Lucic, "Recent Advances in Autoencoder-Based Representation
1401 Learning," Dec. 2018, doi: 10.48550/arxiv.1812.05069.
- 1402 [184] M. Tschannen, O. Bachem, and M. Lucic, "Recent Advances in Autoencoder-Based Representation
1403 Learning," Dec. 2018, doi: 10.48550/arxiv.1812.05069.
- 1404 [185] J. Amin *et al.*, "Brain Tumor Detection by Using Stacked Autoencoders in Deep Learning," *Journal*
1405 *of Medical Systems 2019 44:2*, vol. 44, no. 2, pp. 1–12, Dec. 2019, doi: 10.1007/S10916-019-1483-
1406 2.
- 1407 [186] M. M. Badža and M. Barjaktarović, "Segmentation of Brain Tumors from MRI Images Using
1408 Convolutional Autoencoder," *Applied Sciences 2021, Vol. 11, Page 4317*, vol. 11, no. 9, p. 4317,
1409 May 2021, doi: 10.3390/APP11094317.
- 1410 [187] J. N. Stember and H. Shalu, "Deep Reinforcement Learning with Automated Label Extraction from
1411 Clinical Reports Accurately Classifies 3D MRI Brain Volumes," *Journal of Digital Imaging 2022*,
1412 pp. 1–10, May 2022, doi: 10.1007/S10278-022-00644-5.
- 1413 [188] R. Dey and F. M. Salemt, "Gate-variants of Gated Recurrent Unit (GRU) neural networks," *Midwest*
1414 *Symposium on Circuits and Systems*, vol. 2017-Augus, pp. 1597–1600, Sep. 2017, doi:
1415 10.1109/MWSCAS.2017.8053243.

- 1416 [189] A. M. G. Allah, A. M. Sarhan, and N. M. Elshennawy, "Classification of Brain MRI Tumor Images
1417 Based on Deep Learning PGGAN Augmentation," *Diagnostics* 2021, Vol. 11, Page 2343, vol. 11,
1418 no. 12, p. 2343, Dec. 2021, doi: 10.3390/DIAGNOSTICS11122343.
- 1419 [190] J. Chang *et al.*, "A mix-pooling CNN architecture with FCRF for brain tumor segmentation," *J Vis*
1420 *Commun Image Represent*, vol. 58, pp. 316–322, Jan. 2019, doi: 10.1016/J.JVCIR.2018.11.047.
- 1421 [191] H. N. T. K. Kaldera, S. R. Gunasekara, and M. B. DIssanayake, "Brain tumor Classification and
1422 Segmentation using Faster R-CNN," *2019 Advances in Science and Engineering Technology*
1423 *International Conferences, ASET 2019*, May 2019, doi: 10.1109/ICASET.2019.8714263.
- 1424 [192] M. Sajjad, S. Khan, K. Muhammad, W. Wu, A. Ullah, and S. W. Baik, "Multi-grade brain tumor
1425 classification using deep CNN with extensive data augmentation," *J Comput Sci*, vol. 30, pp. 174–
1426 182, Jan. 2019, doi: 10.1016/J.JOCS.2018.12.003.
- 1427 [193] M. Y. B. Murthy, A. Koteswararao, and M. S. Babu, "Adaptive fuzzy deformable fusion and
1428 optimized CNN with ensemble classification for automated brain tumor diagnosis," *Biomedical*
1429 *Engineering Letters* 2021 12:1, vol. 12, no. 1, pp. 37–58, Nov. 2021, doi: 10.1007/S13534-021-
1430 00209-5.
- 1431 [194] A. Rehman, M. A. Khan, T. Saba, Z. Mehmood, U. Tariq, and N. Ayesha, "Microscopic brain tumor
1432 detection and classification using 3D CNN and feature selection architecture," *Microsc Res Tech*,
1433 vol. 84, no. 1, pp. 133–149, Jan. 2021, doi: 10.1002/JEMT.23597.
- 1434 [195] J. Amin, M. Sharif, M. Raza, T. Saba, R. Sial, and S. A. Shad, "Brain tumor detection: a long short-
1435 term memory (LSTM)-based learning model," *Neural Computing and Applications* 2019 32:20, vol.
1436 32, no. 20, pp. 15965–15973, Dec. 2019, doi: 10.1007/S00521-019-04650-7.
- 1437 [196] G. Liu, X. Li, and Y. Cai, "Segmentation for Multimodal Brain Tumor Images Using Dual-Tree
1438 Complex Wavelet Transform and Deep Reinforcement Learning," *Comput Intell Neurosci*, vol.
1439 2022, pp. 1–11, May 2022, doi: 10.1155/2022/5369516.
- 1440 [197] T. Sathies Kumar, C. Arun, and P. Ezhumalai, "An approach for brain tumor detection using optimal
1441 feature selection and optimized deep belief network," *Biomed Signal Process Control*, vol. 73, p.
1442 103440, Mar. 2022, doi: 10.1016/J.BSPC.2021.103440.
- 1443 [198] P. Harish and S. Baskar, "MRI based detection and classification of brain tumor using enhanced
1444 faster R-CNN and Alex Net model," *Mater Today Proc*, Dec. 2020, doi:
1445 10.1016/J.MATPR.2020.11.495.
- 1446 [199] B. Ahmad, J. Sun, Q. You, V. Palade, and Z. Mao, "Brain Tumor Classification Using a
1447 Combination of Variational Autoencoders and Generative Adversarial Networks," *Biomedicines*
1448 2022, Vol. 10, Page 223, vol. 10, no. 2, p. 223, Jan. 2022, doi: 10.3390/BIOMEDICINES10020223.
- 1449 [200] D. Mukherkjee, P. Saha, D. Kaplun, A. Sinitca, and R. Sarkar, "Brain tumor image generation using
1450 an aggregation of GAN models with style transfer," *Scientific Reports* 2022 12:1, vol. 12, no. 1, pp.
1451 1–16, Jun. 2022, doi: 10.1038/s41598-022-12646-y.
- 1452 [201] W. Takrouni and A. Douik, "Improving geometric P-norm-based glioma segmentation through deep
1453 convolutional autoencoder encapsulation," *Biomed Signal Process Control*, vol. 71, p. 103232, Jan.
1454 2022, doi: 10.1016/J.BSPC.2021.103232.

- 1455 [202] A. Chattopadhyay and M. Maitra, "MRI-based brain tumour image detection using CNN based deep
1456 learning method," *Neuroscience Informatics*, vol. 2, no. 4, p. 100060, Dec. 2022, doi:
1457 10.1016/J.NEURI.2022.100060.
- 1458 [203] N. Kesav and M. G. Jibukumar, "Efficient and low complex architecture for detection and
1459 classification of Brain Tumor using RCNN with Two Channel CNN," *Journal of King Saud*
1460 *University - Computer and Information Sciences*, May 2021, doi: 10.1016/J.JKSUCI.2021.05.008.
- 1461 [204] R. Vankdothu, M. A. Hameed, and H. Fatima, "A Brain Tumor Identification and Classification
1462 Using Deep Learning based on CNN-LSTM Method," *Computers and Electrical Engineering*, vol.
1463 101, p. 107960, Jul. 2022, doi: 10.1016/J.COMPELECENG.2022.107960.
- 1464 [205] L. Fidon, S. Ourselin, and T. Vercauteren, "Generalized Wasserstein Dice Score, Distributionally
1465 Robust Deep Learning, and Ranger for Brain Tumor Segmentation: BraTS 2020 Challenge,"
1466 *Lecture Notes in Computer Science (including subseries Lecture Notes in Artificial Intelligence and*
1467 *Lecture Notes in Bioinformatics)*, vol. 12659 LNCS, pp. 200–214, 2021, doi: 10.1007/978-3-030-
1468 72087-2_18/COVER/.
- 1469 [206] F. Isensee, P. F. Jäger, P. M. Full, P. Vollmuth, and K. H. Maier-Hein, "nnU-Net for Brain Tumor
1470 Segmentation," *Lecture Notes in Computer Science (including subseries Lecture Notes in Artificial*
1471 *Intelligence and Lecture Notes in Bioinformatics)*, vol. 12659 LNCS, pp. 118–132, 2021, doi:
1472 10.1007/978-3-030-72087-2_11/COVER/.
- 1473 [207] T. Henry *et al.*, "Brain Tumor Segmentation with Self-ensembled, Deeply-Supervised 3D U-Net
1474 Neural Networks: A BraTS 2020 Challenge Solution," *Lecture Notes in Computer Science*
1475 *(including subseries Lecture Notes in Artificial Intelligence and Lecture Notes in Bioinformatics)*,
1476 vol. 12658 LNCS, pp. 327–339, 2021, doi: 10.1007/978-3-030-72084-1_30/COVER/.
- 1477 [208] Y. Yuan, "Automatic Brain Tumor Segmentation with Scale Attention Network," *Lecture Notes in*
1478 *Computer Science (including subseries Lecture Notes in Artificial Intelligence and Lecture Notes in*
1479 *Bioinformatics)*, vol. 12658 LNCS, pp. 285–294, 2021, doi: 10.1007/978-3-030-72084-
1480 1_26/COVER/.
- 1481 [209] J. Tang, T. Li, H. Shu, and H. Zhu, "Variational-Autoencoder Regularized 3D MultiResUNet for
1482 the BraTS 2020 Brain Tumor Segmentation," *Lecture Notes in Computer Science (including*
1483 *subseries Lecture Notes in Artificial Intelligence and Lecture Notes in Bioinformatics)*, vol. 12659
1484 LNCS, pp. 431–440, 2021, doi: 10.1007/978-3-030-72087-2_38/COVER/.
- 1485 [210] C. A. Silva, A. Pinto, S. Pereira, and A. Lopes, "Multi-stage Deep Layer Aggregation for Brain
1486 Tumor Segmentation," *Lecture Notes in Computer Science (including subseries Lecture Notes in*
1487 *Artificial Intelligence and Lecture Notes in Bioinformatics)*, vol. 12659 LNCS, pp. 179–188, 2021,
1488 doi: 10.1007/978-3-030-72087-2_16/COVER/.
- 1489 [211] T. Tarasiewicz, M. Kawulok, and J. Nalepa, "Lightweight U-Nets for Brain Tumor Segmentation,"
1490 *Lecture Notes in Computer Science (including subseries Lecture Notes in Artificial Intelligence and*
1491 *Lecture Notes in Bioinformatics)*, vol. 12659 LNCS, pp. 3–14, 2021, doi: 10.1007/978-3-030-
1492 72087-2_1/COVER/.
- 1493 [212] S. Qamar, P. Ahmad, and L. Shen, "HI-Net: Hyperdense Inception 3D UNet for Brain Tumor
1494 Segmentation," *Lecture Notes in Computer Science (including subseries Lecture Notes in Artificial*

- 1495 *Intelligence and Lecture Notes in Bioinformatics*), vol. 12659 LNCS, pp. 50–57, 2021, doi:
1496 10.1007/978-3-030-72087-2_5/COVER/.
- 1497 [213] P. Ahmad, S. Qamar, L. Shen, and A. Saeed, “Context Aware 3D UNet for Brain Tumor
1498 Segmentation,” *Lecture Notes in Computer Science (including subseries Lecture Notes in Artificial
1499 Intelligence and Lecture Notes in Bioinformatics)*, vol. 12658 LNCS, pp. 207–218, 2021, doi:
1500 10.1007/978-3-030-72084-1_19/COVER/.
- 1501 [214] J. Colman, L. Zhang, W. Duan, and X. Ye, “DR-Unet104 for Multimodal MRI Brain Tumor
1502 Segmentation,” *Lecture Notes in Computer Science (including subseries Lecture Notes in Artificial
1503 Intelligence and Lecture Notes in Bioinformatics)*, vol. 12659 LNCS, pp. 410–419, 2021, doi:
1504 10.1007/978-3-030-72087-2_36/COVER/.
- 1505 [215] Z. Jiang, C. Ding, M. Liu, and D. Tao, “Two-stage cascaded u-net: 1st place solution to brats
1506 challenge 2019 segmentation task,” *Lecture Notes in Computer Science (including subseries Lecture
1507 Notes in Artificial Intelligence and Lecture Notes in Bioinformatics)*, vol. 11992 LNCS, pp. 231–
1508 241, 2020, doi: 10.1007/978-3-030-46640-4_22/COVER/.
- 1509 [216] A. Myronenko and A. Hatamizadeh, “Robust semantic segmentation of brain tumor regions from
1510 3D MRIs,” *Lecture Notes in Computer Science (including subseries Lecture Notes in Artificial
1511 Intelligence and Lecture Notes in Bioinformatics)*, vol. 11993 LNCS, pp. 82–89, 2020, doi:
1512 10.1007/978-3-030-46643-5_8/COVER/.
- 1513 [217] R. R. Agravat and M. S. Raval, “Brain tumor segmentation and survival prediction,” *Lecture Notes
1514 in Computer Science (including subseries Lecture Notes in Artificial Intelligence and Lecture Notes
1515 in Bioinformatics)*, vol. 11992 LNCS, pp. 338–348, 2020, doi: 10.1007/978-3-030-46640-
1516 4_32/COVER/.
- 1517 [218] F. Wang, R. Jiang, L. Zheng, C. Meng, and B. Biswal, “3d u-net based brain tumor segmentation
1518 and survival days prediction,” *Lecture Notes in Computer Science (including subseries Lecture
1519 Notes in Artificial Intelligence and Lecture Notes in Bioinformatics)*, vol. 11992 LNCS, pp. 131–
1520 141, 2020, doi: 10.1007/978-3-030-46640-4_13/COVER/.
- 1521 [219] M. U. Saeed *et al.*, “RMU-Net: A Novel Residual Mobile U-Net Model for Brain Tumor
1522 Segmentation from MR Images,” *Electronics 2021, Vol. 10, Page 1962*, vol. 10, no. 16, p. 1962,
1523 Aug. 2021, doi: 10.3390/ELECTRONICS10161962.
- 1524 [220] G. K. Murugesan *et al.*, “Multidimensional and multiresolution ensemble networks for brain tumor
1525 segmentation,” *Lecture Notes in Computer Science (including subseries Lecture Notes in Artificial
1526 Intelligence and Lecture Notes in Bioinformatics)*, vol. 11993 LNCS, pp. 148–157, 2020, doi:
1527 10.1007/978-3-030-46643-5_14/COVER/.
- 1528 [221] Y. X. Zhao, Y. M. Zhang, and C. L. Liu, “Bag of tricks for 3d mri brain tumor segmentation,”
1529 *Lecture Notes in Computer Science (including subseries Lecture Notes in Artificial Intelligence and
1530 Lecture Notes in Bioinformatics)*, vol. 11992 LNCS, pp. 210–220, 2020, doi: 10.1007/978-3-030-
1531 46640-4_20/COVER/.
- 1532 [222] M. Amian and M. Soltaninejad, “Multi-resolution 3d cnn for mri brain tumor segmentation and
1533 survival prediction,” *Lecture Notes in Computer Science (including subseries Lecture Notes in
1534 Artificial Intelligence and Lecture Notes in Bioinformatics)*, vol. 11992 LNCS, pp. 221–230, 2020,
1535 doi: 10.1007/978-3-030-46640-4_21/COVER/.

- 1536 [223] M. Bhalerao and S. Thakur, "Brain tumor segmentation based on 3D residual U-Net," *Lecture Notes*
1537 *in Computer Science (including subseries Lecture Notes in Artificial Intelligence and Lecture Notes*
1538 *in Bioinformatics)*, vol. 11993 LNCS, pp. 218–225, 2020, doi: 10.1007/978-3-030-46643-
1539 5_21/COVER/.
- 1540 [224] J. Sun, Y. Peng, Y. Guo, and D. Li, "Segmentation of the multimodal brain tumor image used the
1541 multi-pathway architecture method based on 3D FCN," *Neurocomputing*, vol. 423, pp. 34–45, Jan.
1542 2021, doi: 10.1016/J.NEUCOM.2020.10.031.
- 1543 [225] L. Weninger, O. Rippel, S. Koppers, and D. Merhof, "Segmentation of brain tumors and patient
1544 survival prediction: Methods for the braTS 2018 challenge," *Lecture Notes in Computer Science*
1545 *(including subseries Lecture Notes in Artificial Intelligence and Lecture Notes in Bioinformatics)*,
1546 vol. 11384 LNCS, pp. 3–12, 2019, doi: 10.1007/978-3-030-11726-9_1/COVER/.
- 1547 [226] C. Zhou, S. Chen, C. Ding, and D. Tao, "Learning contextual and attentive information for brain
1548 tumor segmentation," *Lecture Notes in Computer Science (including subseries Lecture Notes in*
1549 *Artificial Intelligence and Lecture Notes in Bioinformatics)*, vol. 11384 LNCS, pp. 497–507, 2019,
1550 doi: 10.1007/978-3-030-11726-9_44/COVER/.
- 1551 [227] R. Mehta and T. Arbel, "3D U-Net for brain tumour segmentation," *Lecture Notes in Computer*
1552 *Science (including subseries Lecture Notes in Artificial Intelligence and Lecture Notes in*
1553 *Bioinformatics)*, vol. 11384 LNCS, pp. 254–266, 2019, doi: 10.1007/978-3-030-11726-
1554 9_23/COVER/.
- 1555 [228] H. Y. Yang and J. Yang, "Automatic brain tumor segmentation with contour aware residual network
1556 and adversarial training," *Lecture Notes in Computer Science (including subseries Lecture Notes in*
1557 *Artificial Intelligence and Lecture Notes in Bioinformatics)*, vol. 11384 LNCS, pp. 267–278, 2019,
1558 doi: 10.1007/978-3-030-11726-9_24/COVER/.
- 1559 [229] W. Chen, B. Liu, S. Peng, J. Sun, and X. Qiao, "S3D-UNET: Separable 3D U-Net for brain tumor
1560 segmentation," *Lecture Notes in Computer Science (including subseries Lecture Notes in Artificial*
1561 *Intelligence and Lecture Notes in Bioinformatics)*, vol. 11384 LNCS, pp. 358–368, 2019, doi:
1562 10.1007/978-3-030-11726-9_32/COVER/.
- 1563 [230] N. M. Aboelenein, P. Songhao, A. Koubaa, A. Noor, and A. Afifi, "HTTU-Net: Hybrid Two Track
1564 U-Net for Automatic Brain Tumor Segmentation," *IEEE Access*, vol. 8, pp. 101406–101415, 2020,
1565 doi: 10.1109/ACCESS.2020.2998601.
- 1566 [231] A. Myronenko, "3D MRI brain tumor segmentation using autoencoder regularization," *Lecture*
1567 *Notes in Computer Science (including subseries Lecture Notes in Artificial Intelligence and Lecture*
1568 *Notes in Bioinformatics)*, vol. 11384 LNCS, pp. 311–320, 2019, doi: 10.1007/978-3-030-11726-
1569 9_28/COVER/.
- 1570 [232] D. Lachinov, E. Vasiliev, and V. Turlapov, "Glioma segmentation with cascaded UNet," *Lecture*
1571 *Notes in Computer Science (including subseries Lecture Notes in Artificial Intelligence and Lecture*
1572 *Notes in Bioinformatics)*, vol. 11384 LNCS, pp. 189–198, 2019, doi: 10.1007/978-3-030-11726-
1573 9_17/COVER/.
- 1574 [233] G. Wang, W. Li, S. Ourselin, and T. Vercauteren, "Automatic Brain Tumor Segmentation Based on
1575 Cascaded Convolutional Neural Networks With Uncertainty Estimation," *Front Comput Neurosci*,
1576 vol. 13, p. 56, Aug. 2019, doi: 10.3389/FNCOM.2019.00056/BIBTEX.

- 1577 [234] G. Wang, W. Li, S. Ourselin, and T. Vercauteren, "Automatic brain tumor segmentation using
1578 convolutional neural networks with test-time augmentation," *Lecture Notes in Computer Science*
1579 *(including subseries Lecture Notes in Artificial Intelligence and Lecture Notes in Bioinformatics)*,
1580 vol. 11384 LNCS, pp. 61–72, 2019, doi: 10.1007/978-3-030-11726-9_6/COVER/.
- 1581 [235] F. Isensee, P. Kickingereder, W. Wick, M. Bendszus, and K. H. Maier-Hein, "Brain tumor
1582 segmentation and radiomics survival prediction: Contribution to the BRATS 2017 challenge,"
1583 *Lecture Notes in Computer Science (including subseries Lecture Notes in Artificial Intelligence and*
1584 *Lecture Notes in Bioinformatics)*, vol. 10670 LNCS, pp. 287–297, 2018, doi: 10.1007/978-3-319-
1585 75238-9_25/COVER/.
- 1586 [236] M. Soltaninejad, L. Zhang, T. Lambrou, G. Yang, N. Allinson, and X. Ye, "MRI brain tumor
1587 segmentation and patient survival prediction using random forests and fully convolutional
1588 networks," *Lecture Notes in Computer Science (including subseries Lecture Notes in Artificial*
1589 *Intelligence and Lecture Notes in Bioinformatics)*, vol. 10670 LNCS, pp. 204–215, 2018, doi:
1590 10.1007/978-3-319-75238-9_18/COVER/.
- 1591 [237] M. Rezaei *et al.*, "A conditional adversarial network for semantic segmentation of brain tumor,"
1592 *Lecture Notes in Computer Science (including subseries Lecture Notes in Artificial Intelligence and*
1593 *Lecture Notes in Bioinformatics)*, vol. 10670 LNCS, pp. 241–252, 2018, doi: 10.1007/978-3-319-
1594 75238-9_21/COVER/.
- 1595 [238] G. Wang, W. Li, S. Ourselin, and T. Vercauteren, "Automatic brain tumor segmentation using
1596 cascaded anisotropic convolutional neural networks," *Lecture Notes in Computer Science (including*
1597 *subseries Lecture Notes in Artificial Intelligence and Lecture Notes in Bioinformatics)*, vol. 10670
1598 LNCS, pp. 178–190, 2018, doi: 10.1007/978-3-319-75238-9_16/COVER/.
- 1599 [239] K. Kamnitsas *et al.*, "Ensembles of multiple models and architectures for robust brain tumour
1600 segmentation," *Lecture Notes in Computer Science (including subseries Lecture Notes in Artificial*
1601 *Intelligence and Lecture Notes in Bioinformatics)*, vol. 10670 LNCS, pp. 450–462, 2018, doi:
1602 10.1007/978-3-319-75238-9_38/COVER/.
- 1603 [240] M. Shaikh, G. Anand, G. Acharya, A. Amrutkar, V. Alex, and G. Krishnamurthi, "Brain tumor
1604 segmentation using dense fully convolutional neural network," *Lecture Notes in Computer Science*
1605 *(including subseries Lecture Notes in Artificial Intelligence and Lecture Notes in Bioinformatics)*,
1606 vol. 10670 LNCS, pp. 309–319, 2018, doi: 10.1007/978-3-319-75238-9_27/COVER/.
- 1607 [241] H. Li, A. Li, and M. Wang, "A novel end-to-end brain tumor segmentation method using improved
1608 fully convolutional networks," *Comput Biol Med*, vol. 108, pp. 150–160, May 2019, doi:
1609 10.1016/J.COMPBIOMED.2019.03.014.
- 1610 [242] M. Islam and H. Ren, "Multi-modal PixelNet for brain tumor segmentation," *Lecture Notes in*
1611 *Computer Science (including subseries Lecture Notes in Artificial Intelligence and Lecture Notes in*
1612 *Bioinformatics)*, vol. 10670 LNCS, pp. 298–308, 2018, doi: 10.1007/978-3-319-75238-
1613 9_26/COVER/.
- 1614 [243] S. Sedlar, "Brain tumor segmentation using a multi-path CNN based method," *Lecture Notes in*
1615 *Computer Science (including subseries Lecture Notes in Artificial Intelligence and Lecture Notes in*
1616 *Bioinformatics)*, vol. 10670 LNCS, pp. 403–422, 2018, doi: 10.1007/978-3-319-75238-
1617 9_35/COVER/.

1618 [244] A. Phophalia and P. Maji, “Multimodal brain tumor segmentation using ensemble of forest method,”
1619 *Lecture Notes in Computer Science (including subseries Lecture Notes in Artificial Intelligence and*
1620 *Lecture Notes in Bioinformatics)*, vol. 10670 LNCS, pp. 159–168, 2018, doi: 10.1007/978-3-319-
1621 75238-9_14/COVER/.

1622